UNIVERSITY OF BIRMINGHAM
University of Birmingham Research at Birmingham

Substrate-gated docking of pore subunit Tha4 in the TatC cavity initiates Tat translocase assembly

Aldridge, Cassie; Ma, Xianyue; Gerard, Fabien; Cline, Kenneth

DOI:
10.1083/jcb.201311057

License:
Creative Commons: Attribution-NonCommercial-ShareAlike (CC BY-NC-SA)

Document Version
Publisher's PDF, also known as Version of record

Citation for published version (Harvard):
Aldridge, C, Ma, X, Gerard, F & Cline, K 2014, 'Substrate-gated docking of pore subunit Tha4 in the TatC cavity initiates Tat translocase assembly', *Journal of Cell Biology*, vol. 205, no. 1, pp. 51-65.
https://doi.org/10.1083/jcb.201311057

Link to publication on Research at Birmingham portal

Publisher Rights Statement:
Checked for eligibility: 10/01/2018

General rights
Unless a licence is specified above, all rights (including copyright and moral rights) in this document are retained by the authors and/or the copyright holders. The express permission of the copyright holder must be obtained for any use of this material other than for purposes permitted by law.

•Users may freely distribute the URL that is used to identify this publication.
•Users may download and/or print one copy of the publication from the University of Birmingham research portal for the purpose of private study or non-commercial research.
•User may use extracts from the document in line with the concept of 'fair dealing' under the Copyright, Designs and Patents Act 1988 (?)
•Users may not further distribute the material nor use it for the purposes of commercial gain.

Where a licence is displayed above, please note the terms and conditions of the licence govern your use of this document.

When citing, please reference the published version.

Take down policy
While the University of Birmingham exercises care and attention in making items available there are rare occasions when an item has been uploaded in error or has been deemed to be commercially or otherwise sensitive.

If you believe that this is the case for this document, please contact UBIRA@lists.bham.ac.uk providing details and we will remove access to the work immediately and investigate.

Download date: 07. May. 2024

Published Online: 7 April, 2014 | Supp Info: http://doi.org/10.1083/jcb.201311057
Downloaded from jcb.rupress.org on January 10, 2019

Substrate-gated docking of pore subunit Tha4 in the TatC cavity initiates Tat translocase assembly

Cassie Aldridge, Xianyue Ma, Fabien Gerard, and Kenneth Cline

Horticultural Sciences Department and Plant Molecular and Cellular Biology, University of Florida, Gainesville, FL 32611

The twin-arginine translocase (Tat) transports folded proteins across tightly sealed membranes. cpTatC is the core component of the thylakoid translocase and coordinates transport through interactions with the substrate signal peptide and other Tat components, notably the Tha4 pore-forming component. Here, Cys–Cys matching mapped Tha4 contact sites on cpTatC and assessed the role of signal peptide binding on Tha4 assembly with the cpTatC–Hcf106 receptor complex. Tha4 made contact with a peripheral cpTatC site in nonstimulated membranes. In the translocase, Tha4 made an additional contact within the cup-shaped cavity of cpTatC that likely seeds Tha4 polymerization to form the pore. Substrate binding triggers assembly of Tha4 onto the interior site. We provide evidence that the substrate signal peptide inserts between cpTatC subunits arranged in a manner that conceivably forms an enclosed chamber. The location of the inserted signal peptide and the Tha4–cpTatC contact data suggest a model for signal peptide–gated Tha4 entry into the chamber to form the translocase.

Introduction

Only two known systems transport fully folded proteins across a membrane bilayer, the peroxisomal import system and the twin-arginine translocation (Tat) system. In both, the point of transmembrane passage is transient, flexible, and built of small subunits (Ma et al., 2011; Celedon and Cline, 2013). The Tat system plays essential roles in bacterial pathogenesis and plant photosynthesis, yet the mechanisms involved in its unusual capability have not been fully elucidated (for recent reviews see Fröbel et al., 2012; Palmer and Berks, 2012; Celedon and Cline, 2013). Tat substrates are targeted by signal peptides that consist of an amino-proximal RR motif followed by a hydrophobic helical H-domain (San Miguel et al., 2003; Klein et al., 2012) and a signal peptidase cleavage C domain. cpTatC (TatC in bacteria), the core component of the thylakoid translocase, is a multispanning membrane protein that serves as the primary signal peptide receptor (Alami et al., 2003; Gérard and Cline, 2006). Tha4 (TatA in bacteria) and Hcf106 (TatB in bacteria), both single-spanning membrane proteins, complete the translocase.

The nature and timing of interactions among Tat components appears critical for allowing on-demand transport while avoiding uncontrolled breach of membrane integrity. In the absence of transport, thylakoid Tat components are organized into two types of complexes; a large receptor complex of ~8 copies each of cpTatC and Hcf106, and separate small Tha4 complexes. Signal peptide binding and the proton gradient trigger Tha4 to assemble with the receptor complex (Mori and Cline, 2002) and "polymerize" (Dabney-Smith et al., 2006) into a homo-oligomer that appears to form the translocation pore (Fröbel et al., 2011; Pal et al., 2013). Fluorescence imaging of TatA (Leake et al., 2008), disulfide cross-linking of Tha4 (Dabney-Smith and Cline, 2009), and thylakoid transport kinetics (Celedon and Cline, 2012) estimate the transport-active oligomer to be 20–25 Tha4 (TatA) subunits. After protein transport, the translocase dissociates (Mori and Cline, 2002). Recent fluorescent imaging studies demonstrate that the *Escherichia coli* Tat system also reversibly assembles the translocase in the presence of substrate and the proton-motive force (Alcock et al., 2013; Rose et al., 2013).

The NMR structure of bacterial TatA (Hu et al., 2010; Rodriguez et al., 2013) shows an L-shaped molecule consisting of an N-terminal transmembrane domain (TM), a hinge, and an amphipathic α-helix (APH). Structural analysis and molecular dynamics simulation of *E. coli* TatA oligomers portray pinwheel structures with the TMs forming the axle and the APHs as spokes draped across the membrane surface (Rodriguez et al., 2013). Interestingly, these analyses suggest that TatA (Tha4) oligomers of

C. Aldridge and X. Ma contributed equally to this paper.

Correspondence to Kenneth Cline: kcline@ufl.edu

Abbreviations used in this paper: APH, amphipathic α-helix; BMOE, bismaleimidoethane; CuP, copper phenanthroline; DSP, dithiobis[succinimidyl propionate]; Tat, twin-arginine translocation; TM, transmembrane domain.

© 2014 Aldridge et al. This article is distributed under the terms of an Attribution–Noncommercial–Share Alike–No Mirror Sites license for the first six months after the publication date (see http://www.rupress.org/terms). After six months it is available under a Creative Commons License (Attribution–Noncommercial–Share Alike 3.0 Unported license, as described at http://creativecommons.org/licenses/by-nc-sa/3.0/).

The Rockefeller University Press $30.00
J. Cell Biol. Vol. 205 No. 1 51–65
www.jcb.org/cgi/doi/10.1083/jcb.201311057

9–25 subunits would create an unstable bilayer structure due to hydrophobic mismatch. Thus, a translocase organization that can enable formation of such oligomers could theoretically harness the instability for translocation of the folded substrate.

Several studies suggest that cpTatC (TatC) serves as organizing center for the translocase. cpTatC (TatC) binds the signal peptide RR domain (Rollauer et al., 2012; Zoufaly et al., 2012; Ma and Cline, 2013). The TatC TM5 binds the TatB TM (Kneuper et al., 2012; Rollauer et al., 2012), and TatB (Hcf106) in turn contacts the signal peptide H-domain (Alami et al., 2003; Gérard and Cline, 2006). TatC also forms cross-links to TatA (Fröbel et al., 2011; Zoufaly et al., 2012), but the site of Tha4 (TatA) translocase assembly is not known. The crystal structure of TatC from *Aquifex aeolicus* provides some clues as to how TatC may organize the translocase (Rollauer et al., 2012; Ramasamy et al., 2013). The monomeric TatC has six TM helices folded into the shape of a cup or glove, and producing a striking concave cavity suggested to be the TatA (Tha4) assembly site (Rollauer et al., 2012) and/or the signal peptide insertion site (Ramasamy et al., 2013). The arrangement of cpTatC (TatC) subunits also appears to be critical to translocase function, as cpTatC mutations that disrupt receptor complex assembly also impair substrate binding (Ma and Cline, 2013). Genetic evidence indicates that a TatC dimer forms the minimal functional unit (Maldonado et al., 2011) and cross-linked dimers of TatC (cpTatC) have been reported (Lee et al., 2006; Zoufaly et al., 2012; Ma and Cline, 2013). However, the arrangement of TatC subunits in such dimers is unclear.

The objectives in the present work were to map the Tha4 assembly site on cpTatC in the translocase and to determine where the signal peptide of bound substrate inserts with respect to cpTatC. The intention was to gain insight into one of the unsolved mysteries of the Tat mechanism: how signal peptide binding provokes Tha4 assembly and polymerization to generate an active translocase. Here we provide evidence for how these two events are linked. We used Cys–Cys matching to map the Tha4 contact site(s) on cpTatC. We found that in the absence of substrate and the proton gradient, Tha4 makes contact with the periphery of the cpTatC cup, very near to the predicted binding site of Hcf106 on TM5 (Kneuper et al., 2012; Rollauer et al., 2012). Upon assembly of the translocase, Tha4 makes enhanced contact with TM5 and also makes contact with a new site in the interior cavity of the cup, which presumably seeds Tha4 polymerization that leads to translocation. We provide evidence that cpTatC subunits are oriented in a concave face-to-face arrangement that could conceivably create a closed chamber, thereby preventing Tha4 access. Upon substrate binding, the signal peptide appears to insert into a space between the cpTatC subunits, which might wedge the edges of the chamber apart to allow Tha4 entry. Alternatively, signal peptide binding to the Hcf106 TM might transiently draw Hcf106 away from TM5 and allow Tha4 entry. A model for translocase assembly is presented.

Results

Because of the transient nature of the assembled translocase, we used C-terminally truncated substrate proteins to increase the lifetime of the translocase. These substrates bind to the receptor complex and trigger Tha4 assembly but do not dissociate from the receptor, nor are they transported (Fig. S1). The truncated substrates were prepared from tOE17-20F, a modified version of the OE17 precursor protein that contains a phenylalanine substitution that reproduces the bacterial twin-arginine consensus motif (R-R-X-F). tOE17-20F has a very high and specific affinity (K_d ~1 nM) for the receptor complex (Celedon and Cline, 2012). The studies below interchangeably used truncated versions with either 12 (SpF12) or 16 (SpF16) mature domain residues. All substrates, except as designated in Fig. S1 and Fig. S5, contained a wild-type signal peptidase cleavage site.

TM4 of cpTatC contacts the Tha4 TM

Rollauer et al. (2012) postulated that TM4 residue Glu170 of *E. coli* TatC, which is on the concave surface of TatC, hydrogen-bonds to TM Gln8 of *E. coli* TatA during translocase assembly. We used Cys–Cys cross-linking to investigate such an interaction between comparable residues cpTatC Q234 and Tha4 E10. Single Cys substitutions were engineered into cpTatC and Tha4 and the resulting variants were shown to be functional in substrate binding and transport assays (Fig. S2 and Fig. S4; Aldridge et al., 2012; Ma and Cline, 2013). In Fig. 1, cpTatC with a Cys substitution of L231, which is on the same TM4 face and one helical turn removed from Q234, was paired with Tha4 with Cys in different domains (Fig. 1 D). Radiolabeled cpTatC L231C was imported into chloroplasts, and thylakoids obtained from the chloroplasts were incubated with in vitro–translated unlabeled Tha4-Cys and in vitro–translated substrate peptide (see Materials and methods). Reactions were illuminated to generate the proton gradient and assemble the translocase (Celedon and Cline, 2012), copper phenanthroline (CuP) was added to promote disulfide formation, and samples were analyzed by nonreducing SDS-PAGE and fluorography. In this assay, imported cpTatC assembles with a free pool of Hcf106 to form new receptor complexes, is fully functional, and is distinguishable from endogenous cpTatC (Ma and Cline, 2013). Added Tha4 is fully functional and present at ~10 times the amount of endogenous Tha4 (Dabney-Smith et al., 2003; Celedon and Cline, 2012). We cannot presently incorporate significant amounts of exogenous Hcf106 into the receptor complex, but Hcf106 contains no Cys residues and cannot participate in disulfide cross-linking reactions.

Cys–Cys cross-links occurred between cpTatC L231C and Tha4 with cysteines in the lumen-proximal TM (Fig. 1 A, lanes 2–4). Cross-links are evident by a characteristic size-shifted cpTatC band at M_r ~42 kD, which equals the sum of cpTatC (M_r 28 kD) plus Tha4 (M_r 14 kD) and which disappears upon disulfide reduction (Fig. 1 A, lanes 13–15). Because Tha4 is unlabeled, it can only be detected through cross-linking and size shifting of the radiolabeled cpTatC. No cross-links were observed between cpTatC and Tha4 with cysteines in the stromal domains (Fig. 1 A, lanes 5–10) or with Tha4 F4C E10Q (lane 11), a nonfunctional mutant that cannot assemble the translocase (Dabney-Smith et al., 2003). The appearance of the 42-kD cross-link band required the SpF16 substrate peptide (Fig. 1 B, compare lanes 1 and 3 with lanes 2 and 4). It is also induced by the full-size substrate tOE17-20F (Fig. 1 C, lane 1) but not by the inactive substrate KK-tOE17-20F (lane 2). These

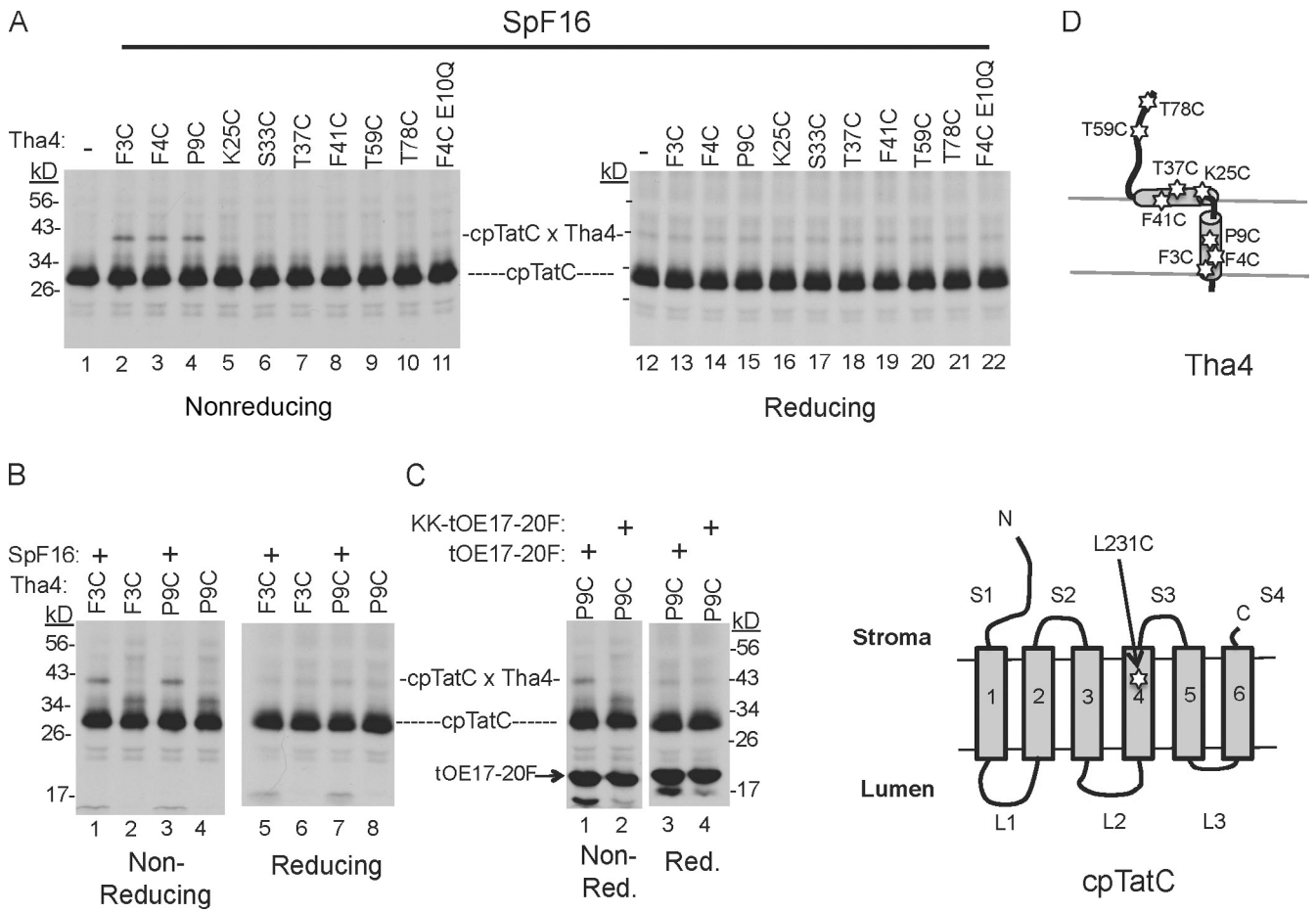

Figure 1. **Contact between the Tha4 TM and cpTatC TM4 in the translocase.** (A) Radiolabeled pre-cpTatC L231C was imported into chloroplasts. Recovered thylakoids were incubated with in vitro–translated unlabeled Tha4 single Cys variants (XnC) followed by in vitro–translated SpF16 Tat substrate (see Materials and methods). Samples at 15°C were illuminated to assemble the translocase and CuP was added to promote disulfide formation (Materials and methods). Analysis was by SDS-PAGE/fluorography under nonreducing or reducing (+ β-mercaptoethanol) conditions. (B) Assays received SpF16 or mock translation extract before cross-linking. (C) Assays received either the full-size substrate tOE17-20F or the inactive twin lysine variant (KK-tOE17-20F). (D) Models of Tha4 and cpTatC with the positions of Cys substitutions marked with stars. Tha4 F4C E10Q is a nonfunctional Tha4 variant.

results indicate that cpTatC-Tha4 cross-linking occurs upon assembly of the translocase.

The ~42-kD band is a Tha4-cpTatC adduct

To verify that the 42-kD band is a cross-linking product between Tha4 and cpTatC, a cross-linking reaction was conducted between radiolabeled cpTatC L231C and unlabeled Tha4 P9C. After cross-linking, samples were dissolved with SDS to dissociate all noncovalent associations and were then subjected to immunoprecipitation with antibodies to Tha4 or cpTatC under denaturing conditions (Fig. 2 A). Anti-Tha4 immunoprecipitated the 42-kD cross-linking band (lane 4); anti-cpTatC precipitated both the 42-kD band and the cpTatC band (lane 5). Anti-Hcf106 immunoprecipitated neither band, as expected (lane 6). The 42-kD cross-linking band disappeared upon reducing the disulfides and with the anti-Tha4 precipitate was replaced by the cpTatC monomer (lanes 7 and 8).

In a second approach, a cross-linking reaction was conducted in which both Tha4 and cpTatC were radiolabeled and cpTatC contained a C-terminal His_6 tag for purification. After cross-linking, the samples were dissolved with the nondenaturing detergent digitonin and cpTatC-His_6 purified by metal ion affinity chromatography under nondenaturing conditions (see Materials and methods). A 43-kD band (owing to the slightly larger cpTatC-His_6) was present in both the load sample and the purified cpTatC sample, but only if the substrate peptide SpF12 was present during the reaction (Fig. 2 B, compare lanes 2 and 4 with lanes 1 and 3). Interestingly, the purified sample also contained a band migrating at the location of Tha4 dimer. When samples were treated with β-mercaptoethanol, the bands at 43 kD and Tha4 dimer disappeared and a band of Tha4 monomer appeared (lane 6). Together, these experiments verify that the 42-kD band (43 kD for cpTatC-His_6) is a cross-linking adduct between cpTatC and Tha4. The co-purification of a Tha4 dimer under nondenaturing conditions was likely due to its association with the cross-linked Tha4 and is an indication of Tha4 polymerization (Dabney-Smith and Cline, 2009).

Stromal domains of cpTatC are in contact with stromal domains of Tha4; lumenal domains of cpTatC are in contact with lumen-proximal domains of Tha4

A survey of cpTatC-Tha4 contacts was conducted by pairing a variety of cpTatC Cys variants with Tha4 Cys variants most

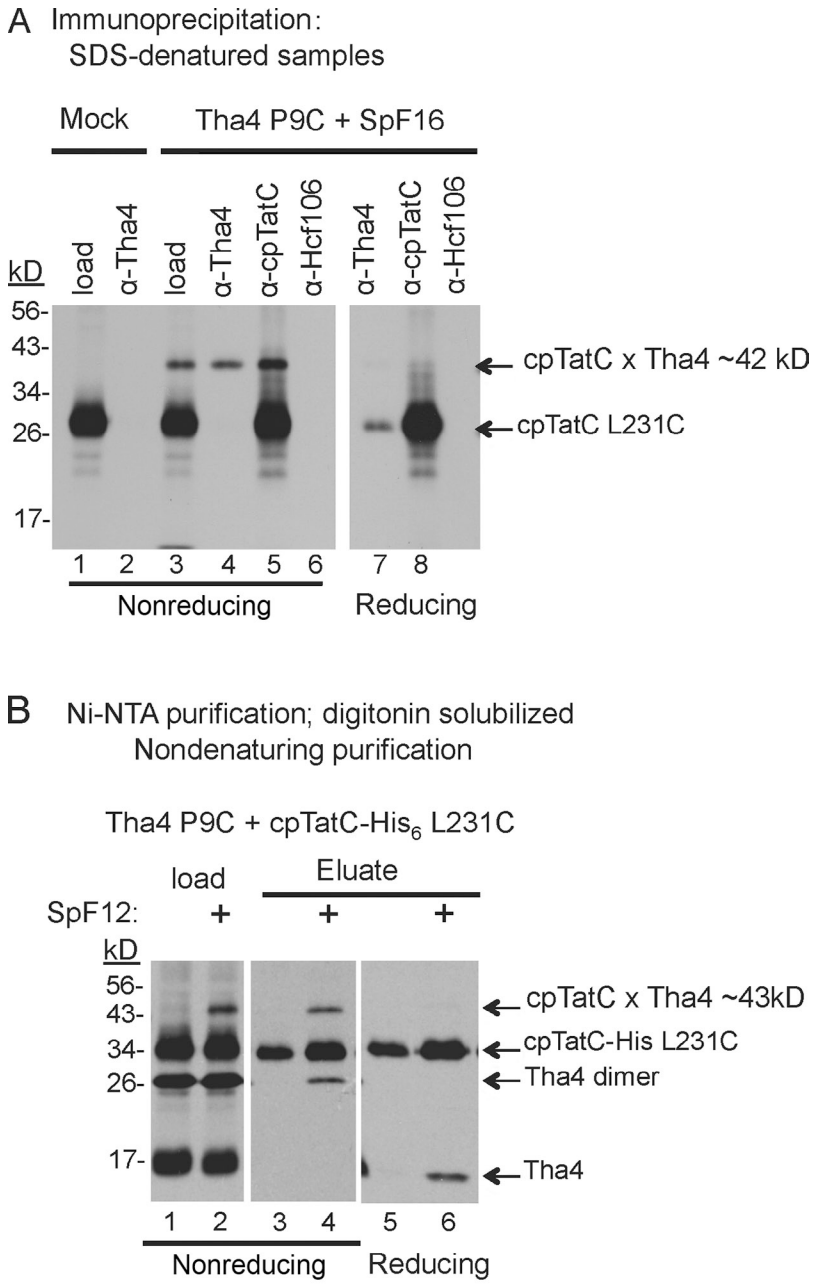

Figure 2. **The ∼42-kD band is a cross-linking product between Tha4 and cpTatC.** (A) Thylakoids with radiolabeled cpTatC L231C were incubated with mock translation extract or unlabeled Tha4 P9C followed by mock translation extract or SpF16. After disulfide cross-linking, recovered thylakoids were subjected to denaturing immunoprecipitation with antibody-linked beads as shown above the panels (see Materials and methods). (B) Thylakoids containing radiolabeled cpTatC–His_6 L231C were incubated with radiolabeled Tha4 P9C and either SpF12 or mock translation extract and then subjected to disulfide cross-linking. Recovered thylakoids were dissolved in 1% digitonin and cpTatC-His_6 purified on magnetic Ni-NTA beads (Materials and methods). Eluted samples in A and B were analyzed by nonreducing or reducing SDS-PAGE/fluorography as in Fig. 1.

likely to form cross-links based on the relative positions of the Cys residues with respect to the membrane (Fig. 3; see Fig. 8 A for a map of cpTatC Cys substitutions). Negative controls for cpTatC with Cys in stroma-exposed or lumen-exposed domains included pairing with a Tha4 Cys exposed to the opposite side of the membrane. An additional negative control included reactions that lacked both Tha4 and substrate (indicated "−" above the panel).

Of cpTatC TM Cys variants tested, only cpTatC L231C (TM4) and cpTatC V270C (TM5) gave cross-linking products with either Tha4 P9C or F3C (Fig. 3, lanes 13, 14, 16, and 17; and Fig. S3 A). We tested additional cpTatC variants with Cys substitutions in TM domains specifically on the concave face of cpTatC (Fig. S4). No significant cross-links were produced. This suggests that the cross-linking via L231C and V270C represents specific interactions because nearly all of the other Cys variants tested were near the middle of the membrane (L146C, Y183, A184, G289, and L287, as is L231C) or lumen-proximal height of the membrane (I98C, C101C, C142C, and L146C, as is V270C). On the other hand, because cpTatC Y259C is located near the stromal surface of TM5, it was also paired with stroma-proximal Tha4 TM residues L20C or V21C (Fig. 4 B) and produced substantial cross-linking with both.

Relatively low amounts of cross-linking product resulted from cpTatC with Cys residues in stroma-facing loops paired with Tha4 with Cys in its APH (Fig. 3 B, lanes 1–12; and Fig. S3 A). Relatively high amounts of cross-linking products were produced from cpTatC with lumen-exposed Cys, e.g., L2 (N203; ∼22%) and L3 (T275C; ∼35%; Fig. 3, lanes 17, 21, and 22; and Fig. S3 A). This high yield of cross-linking may be due to the oxidizing

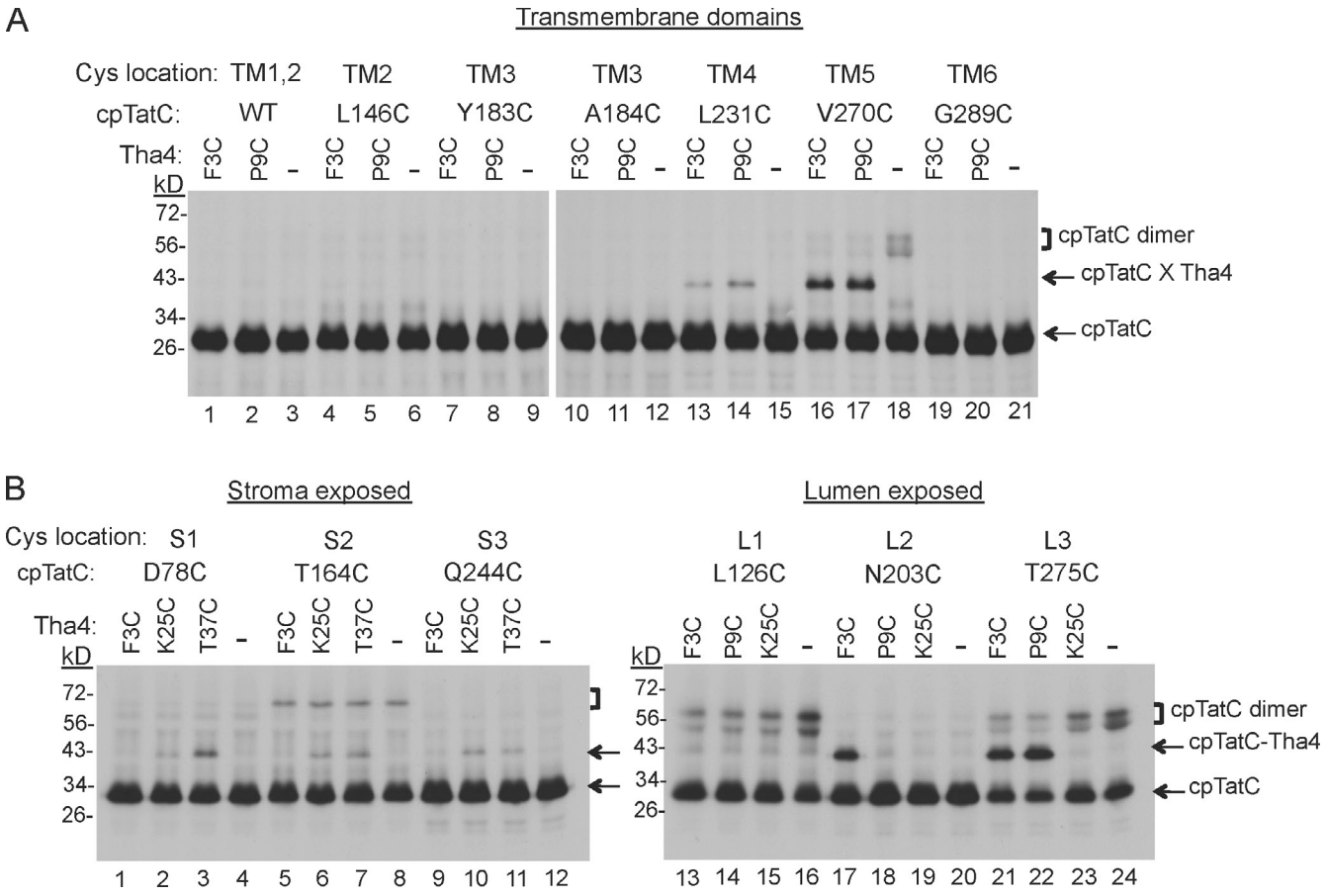

Figure 3. **Stromal domains of cpTatC contact the stromal domain of Tha4; lumenal domains of cpTatC contact the lumen-proximal domain of Tha4.** Thylakoid membranes containing radiolabeled cpTatC single Cys variants were incubated with unlabeled Tha4 single Cys variants and SpF16 or with mock translation extract (−) as in Fig. 1 and subjected to disulfide cross-linking (see Materials and methods). Samples were analyzed by nonreducing SDS-PAGE/fluorography. (A) cpTatC with Cys residues in transmembrane domains. (B) cpTatC with Cys residues in stroma-exposed and lumen-exposed domains.

nature of the lumen. As expected, cross-linking products were not observed for combinations of cpTatC with stroma- or lumen-exposed Cys with Tha4 Cys variants that are exposed on the opposite sides of the membrane (e.g., Fig. 3 B, compare lane 17 with lane 19; Fincher et al., 2003; Aldridge et al., 2012; Koch et al., 2012).

Contact between cpTatC TM4, TM5, and the Tha4 TM is dependent on substrate and the proton gradient; contact between cpTatC L3 and Tha4 is constitutive

Disulfide cross-linking between cpTatC-Tha4 combinations was examined for substrate dependence (Fig. 4 and Fig. S3 B). Cross-linking directed from cpTatC L231C (TM4) was enhanced approximately fivefold by substrate (Fig. 4 A, compare lanes 15 and 17 to lanes 16 and 18; and Fig. S3 B). Cross-linking directed from cpTatC V270C (TM5) or N203C (L2) was enhanced 1.5–2-fold by substrate (Fig. 4 A, lanes 7, 8, and 19–22), and cross-linking directed from the stroma-proximal TM5 residue Y259C and stroma-proximal Tha4 TM residues was enhanced up to fivefold by substrate (Fig. 4 B, lanes 3–6; and Fig. S3 B). cpTatC D78C was the only stromal Cys variant with substrate-enhanced cross-linking (Fig. 4 A, lanes 1 and 2; and Fig. S3 B). By contrast, cross-linking directed by cpTatC L3 T275C was independent of substrate (Fig. 4 A, lanes 11–14; and Fig. S3 B).

As seen in Figs. 3 and 4, putative cpTatC dimers were produced from cpTatC with cysteines in S2, L1, L3, and the lumen-proximal TM5 V270C (Ma and Cline, 2013). The cpTatC dimers directed from the lumen-proximal Cys residues migrated as doublets in some, but not all, experiments (Fig. 4 C). Doublets may relate to the use of CuP, as discrete bands were always obtained when bismaleimidoethane (BMOE) was used to cross-link. As shown in Fig. 4 C, substrate binding substantially reduced dimers directed by either L126C (lanes 1 and 2) or V270C (lanes 4 and 5), but was without effect on dimers directed by L3 T275C (lanes 7 and 8).

The proton gradient initiates assembly of the translocase (Mori and Cline, 2002; Dabney-Smith and Cline, 2009) and reportedly powers thylakoid Tat protein transport (Alder and Theg, 2003). The proton gradient requirement for selected cpTatC-Tha4 pairs was examined by conducting assays in darkness or light, with or without the ionophore combination nigericin/valinomycin (Fig. 5). Ionophores drastically reduced the formation of cpTatC L231C:Tha4 P9C (Fig. 5, A and B, lanes 3 and 2; and Fig. 5 C) and cpTatC Y259C:Tha4 L20C (Fig. 5, A and B, lanes 9 and 8; and Fig. 5 C) and significantly reduced the amount of cross-linking

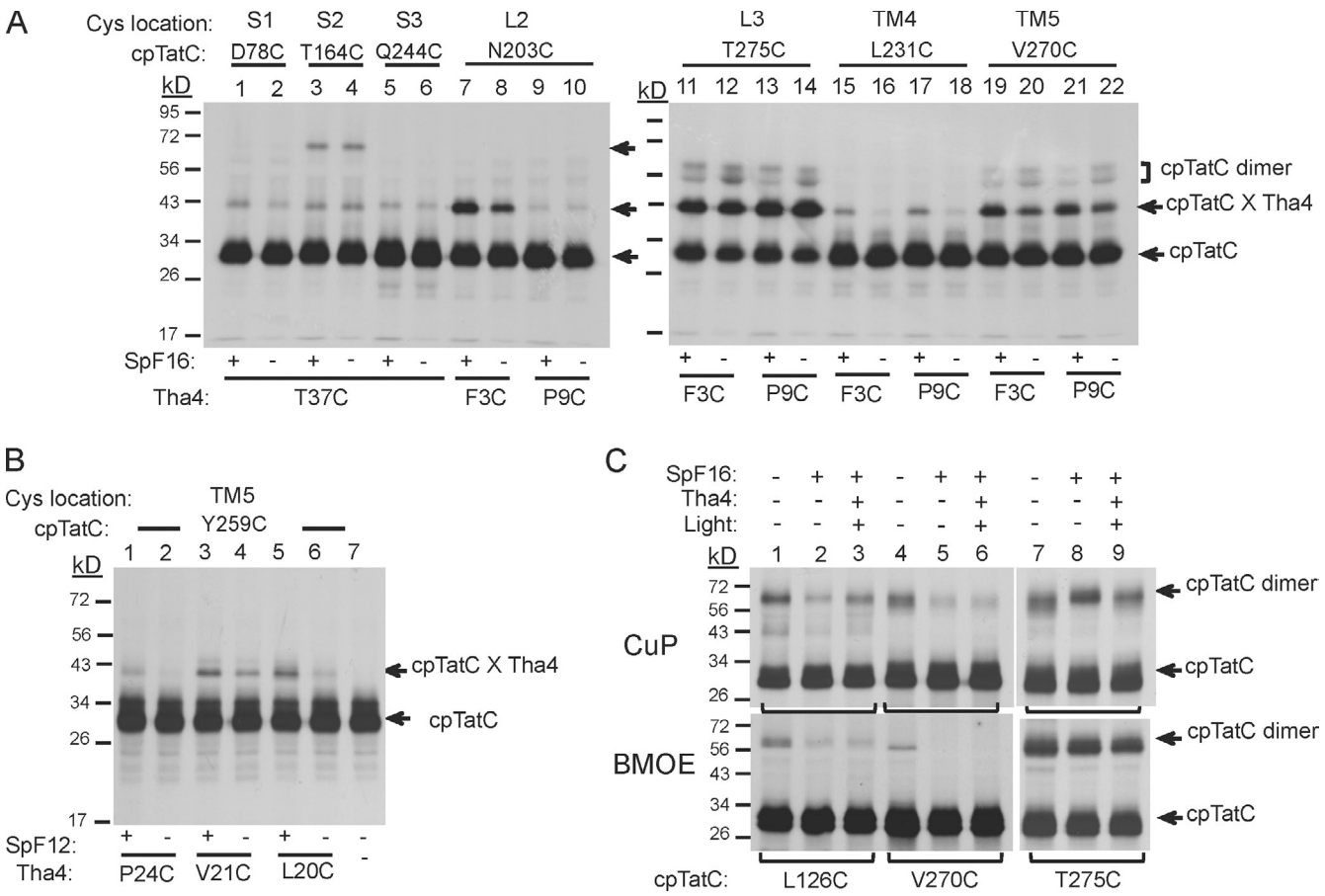

Figure 4. **Tha4 contacts lumenal loop L3 of cpTatC constitutively, and TM4 and TM5 in a substrate-enhanced manner.** (A and B) Thylakoid membranes containing radiolabeled cpTatC Cys received unlabeled Tha4 Cys variants and either mock translation extract (−) or SpF16, and were subjected to disulfide cross-linking (see Materials and methods). (C) The effects of substrate binding and translocase assembly on cpTatC dimerization directed by lumen proximal L126C, V270C, and T275C. Thylakoids with imported radiolabeled cpTatC-Cys were incubated with mock translation extract, unlabeled SpF16 plus mock translation extract, and SpF16 plus unlabeled wild-type Tha4 as shown. Disulfide cross-linking was as in Fig. 1 and BMOE cross-linking as in the Materials and methods, except that only the reactions with Tha4 plus SpF16 received light during the reaction and pre-incubation.

products from cpTatC V270C:Tha4 P9C (Fig. 5, A and B, lanes 5 and 6; and Fig. 5 C). By contrast, ionophores were without effect on cpTatC T275C-Tha4 F4C cross-linking (Fig. 5 D, lanes 6 and 7). cpTatC T275C even efficiently cross-linked to Tha4 F4C E10Q (Fig. 5 D, lane 8).

Unexpectedly, the proton gradient stimulation of cross-linking product was roughly the same regardless of whether the assays were conducted in darkness (Fig. 5 A) or in light (Fig. 5 B), as shown in Fig. 5 C. These results suggests that a large and sustained proton gradient is not needed for the substrate-dependent movement of Tha4, but rather that a residual pool of localized protons is sufficient, i.e., those remaining from the light pretreatment necessary to fully integrate Tha4 (Aldridge et al., 2012; see Materials and methods).

Together, these results show that some Tha4 can contact the cpTatC L3 domain (T275) constitutively, that cpTatC TM4 (L231C) contacts the Tha4 TM only under translocase conditions, and that maximum contact between both ends of the carboxyl-proximal helix of cpTatC TM5 (Y259 and V270) and the Tha4 TM requires substrate and the proton gradient. It is notable that no cross-links resulted from Cys residues on the convex side of cpTatC.

The H-domain of the substrate signal peptide inserts on the concave side of cpTatC

Binding of the signal peptide triggers Tha4 assembly and polymerization (Mori and Cline, 2002; Dabney-Smith et al., 2006; Dabney-Smith and Cline, 2009). The signal peptide RR domain is bound by the cpTatC amino-proximal S1 and S2 domains (Ma and Cline, 2013), but the H/C domain appears to be buried somewhere in the translocase (Gérard and Cline, 2007; Fröbel et al., 2012). We investigated the signal peptide H/C location by disulfide cross-linking of thylakoid-bound single Cys tOE17-20F, i.e., the full-length substrate containing the folded domain (Ma and Cline, 2010, 2013), and single Cys cpTatC. A substrate-cpTatC cross-linking product at the expected 48 kD was only obtained with the cpTatC TM5 residue V270C (Fig. 6 B, lanes 10 and 21; and Fig. 6 C). All other combinations including those in Fig. 6 B and cpTatC I174C (TM3) and cpTatC S228C (TM4) (not depicted) did not produce the 48-kD adduct. The identity of the 48-kD band as a cpTatC-substrate cross-linking product was verified by an experiment (Fig. 6 C) in which only one protein, either cpTatC (lane 4) or substrate (lane 5) was radiolabeled. The 48-kD band was produced in both cases, but

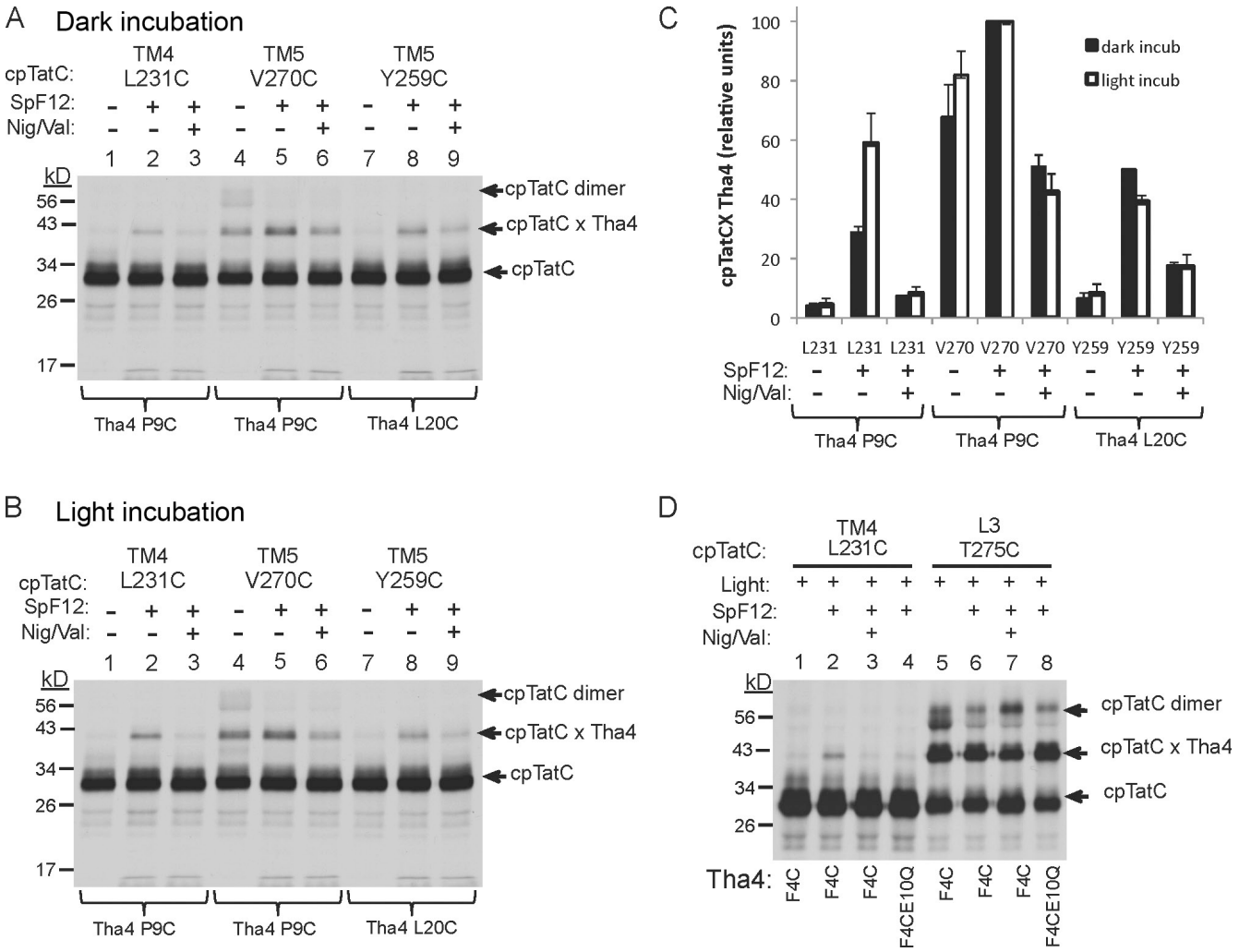

Figure 5. **Substrate-enhanced contacts between the Tha4 TM and cpTatC TM4 and TM5 also require the proton gradient.** Thylakoid membranes containing radiolabeled cpTatC Cys variants in TM4 (L231C), TM5 (Y259C or V270C), or L3 (T275C) were incubated with unlabeled Tha4 Cys variants and mock translation extract or SpF12, and were subjected to disulfide cross-linking. All reactions were preincubated in light during Tha4 integration (see Materials and methods). Incubations for cross-linking in A were in darkness. Incubations in B and D were in the light. As designated by Nig/Val +, certain reactions received 1 µM nigericin and 2 µM valinomycin immediately after SpF12 addition to dissipate the proton gradient. (C) The cpTatC x Tha4 cross-linking products in A and B were quantified by densitometric analysis of films scanned by light transmission and analyzed with ImageJ software. The averages and differences from the mean were from two repeats of the experiment. All values from each film were normalized to the density of the cpTatC V270C × Tha4 P9C plus SpF12 band, which was assigned an arbitrary value of 100.

with the expected reduced radiolabel intensity (compare with lane 3). The range of substrate variants that cross-linked to cpTatC V270C was narrow, with −7C (lane 8) giving much stronger cross-linking than flanking −10C (lane 7) and −4C (lane 9) substrates. This indicates that the signal peptide H-domain inserts on the concave face of cpTatC and is narrowly exposed to the lumen-proximal end of TM5.

Substrate protein signal peptides insert between cpTatC subunits

At saturation there is only one bound substrate per cpTatC (Celedon and Cline, 2012). Because the RR-binding site and the −7C cross-linking site are on distal ends of the cpTatC monomer, the simplest explanation is that the signal peptide −7 position is close to a different cpTatC subunit than the cpTatC subunit that binds the RR domain. This could occur if cpTatC subunits are arranged in a head-to-tail organization as suggested (Rollauer et al., 2012), either in a somewhat linear arrangement or in a concave face-to-face arrangement. As observed in Fig. 6 and previously (Ma and Cline, 2010, 2013), bound substrates containing Cys residues in their signal peptides from position −7 through the first ∼37 residues of the mature OE17 protein form disulfide-linked substrate dimers. Such dimerization is easiest to explain by the face-to-face arrangement.

To investigate this possibility we conducted an experiment to determine if a pair of substrates cross-linked through their dimerization region could simultaneously be cross-linked from their RR-proximal regions to S1 domains of two different cpTatCs. The tOE17-20F substrates contained a Cys substitution at the RR-proximal −25 position and a second Cys substitution in the substrate dimerization region in the signal peptide (−3) or early mature domain (+3 or +17). Substrates were bound to membranes containing cpTatC E73C (S1 domain) and were subjected to disulfide cross-linking with CuP. As shown in Fig. 7, either the

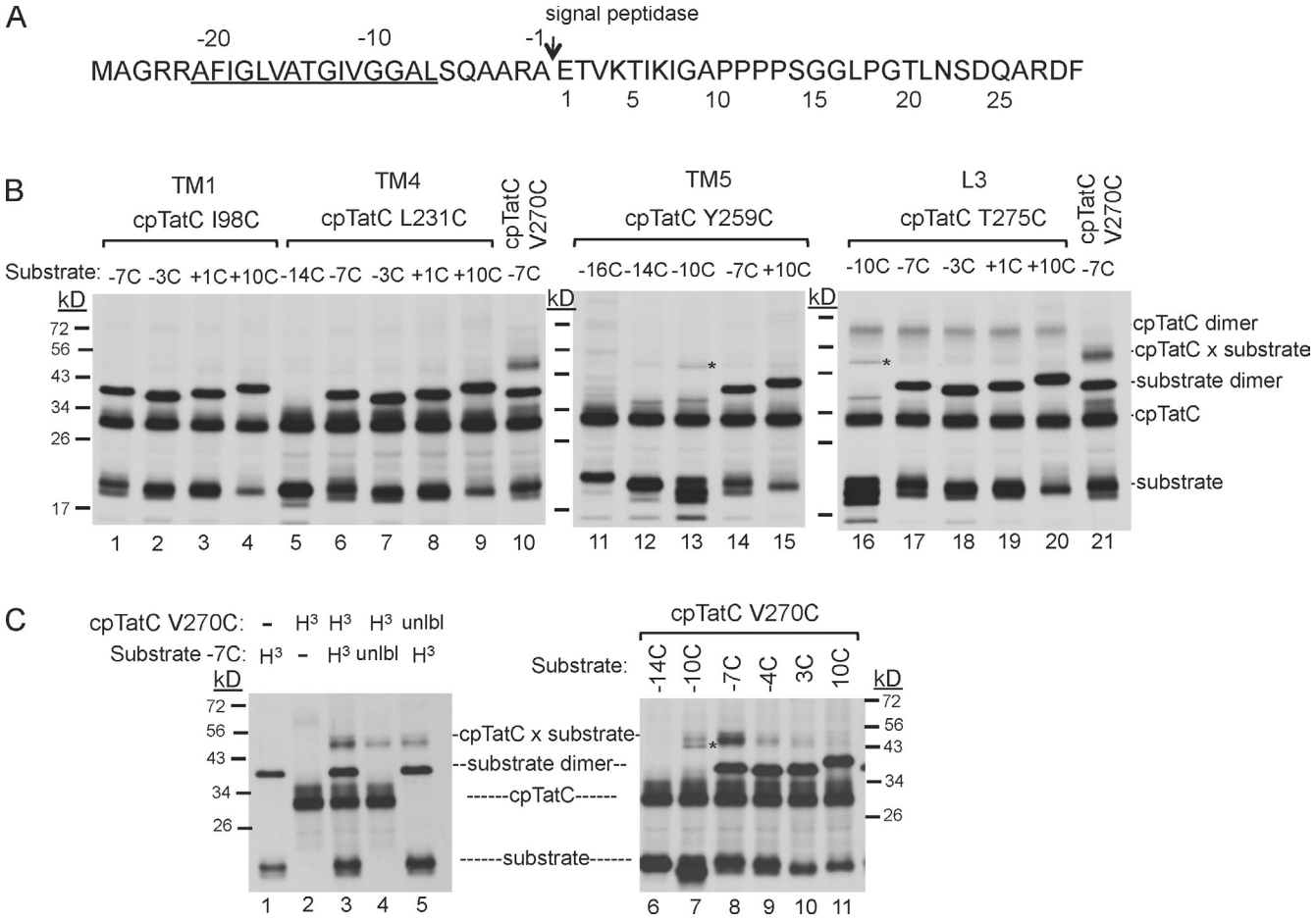

Figure 6. **The H-domain of the substrate signal peptide makes contact with the cpTatC concave surface at TM5.** Thylakoid membranes containing radiolabeled cpTatC Cys variants were incubated in a binding reaction with tOE17-20F substrate Cys variants as shown above the panels. After washing, thylakoids were subjected to disulfide cross-linking at 15°C. (A) Diagram of the signal peptide and early mature domain of the substrate showing numbering convention. The H-domain is underlined. (B) Survey of cpTatC Cys with substrate containing Cys in the signal peptide or early mature domain. (C, left) Demonstration that the ∼48-kD band is a cross-linking product between substrate −7C and cpTatC V270C. Cross-linking reactions were conducted in which substrate or cpTatC-Cys was absent, or in which only one or both were radiolabeled as shown above the panel. (Right) The cpTatC TM5 V270C was combined with substrate containing a range of single Cys substitutions. The ∼46-kD band produced from substrate −10C (asterisk) is a nonspecific cross-linking product.

substrate or the cpTatC are radiolabeled and the other unlabeled, as designated above and below the panels. All three double Cys-substituted substrates produced five substrate-labeled bands when paired with cpTatC E73C (designated B1 through B5; lanes 1, 2, and 10), with the clearest banding pattern occurring with the −25C −3C substrate (lanes 9–13). B1 is the substrate monomer; B2 is the substrate dimer as shown by comparison to the banding for the −3C substrate, which forms dimers but does not cross-link to cpTatC E73C (lane 12). B3 is a 1:1 substrate/cpTatC adduct as shown in lanes 6 and 11, and as reported previously (Ma and Cline, 2013), that the −25C substrate cross-links to cpTatC E73C but does not form substrate dimers. The largest cross-linking product that could be obtained from the combination of −25C −3C substrate and cpTatC E73C would result from two cpTatC subunits individually cross-linked to the −25C positions of a substrate dimer linked through the −3 Cys. The B5 band migrated at the molecular weight expected for such an adduct. B4 migrated as expected for an adduct of two substrates linked to one cpTatC. This assignment was confirmed by an experiment in which cpTatC was labeled with ^{35}S-methionine and substrate with ^{3}H-leucine (lane 13). Quantification of ^{35}S and ^{3}H in bands yielded the expected 1:1 substrate/cpTatC ratio for B5 and 2:1 substrate/cpTatC ratio for B4. Because the −3 position is only 4 residues from the −7 position that contacts TM5 V270C on the concave side of cpTatC (Fig. 6), this result suggests that the signal peptide H-domains of the substrate dimer are inserted between concave faces of at least two cpTatC subunits (Fig. 8 B). A chase experiment (transport of bound precursor) verified that substrate moieties of B5 and B4 undergo transport when the membrane is energized (Fig. S5).

Discussion

This study was undertaken to map component and substrate interactions that occur during Tha4 assembly with the receptor complex to form the active translocase and, in so doing, model the initial steps leading to protein transport. Previous work demonstrated that Tha4 assembly with the cpTatC–Hcf106 receptor requires substrate binding, the proton gradient (Mori and Cline, 2002), and the E10 of Tha4 (Dabney-Smith et al., 2003). Here,

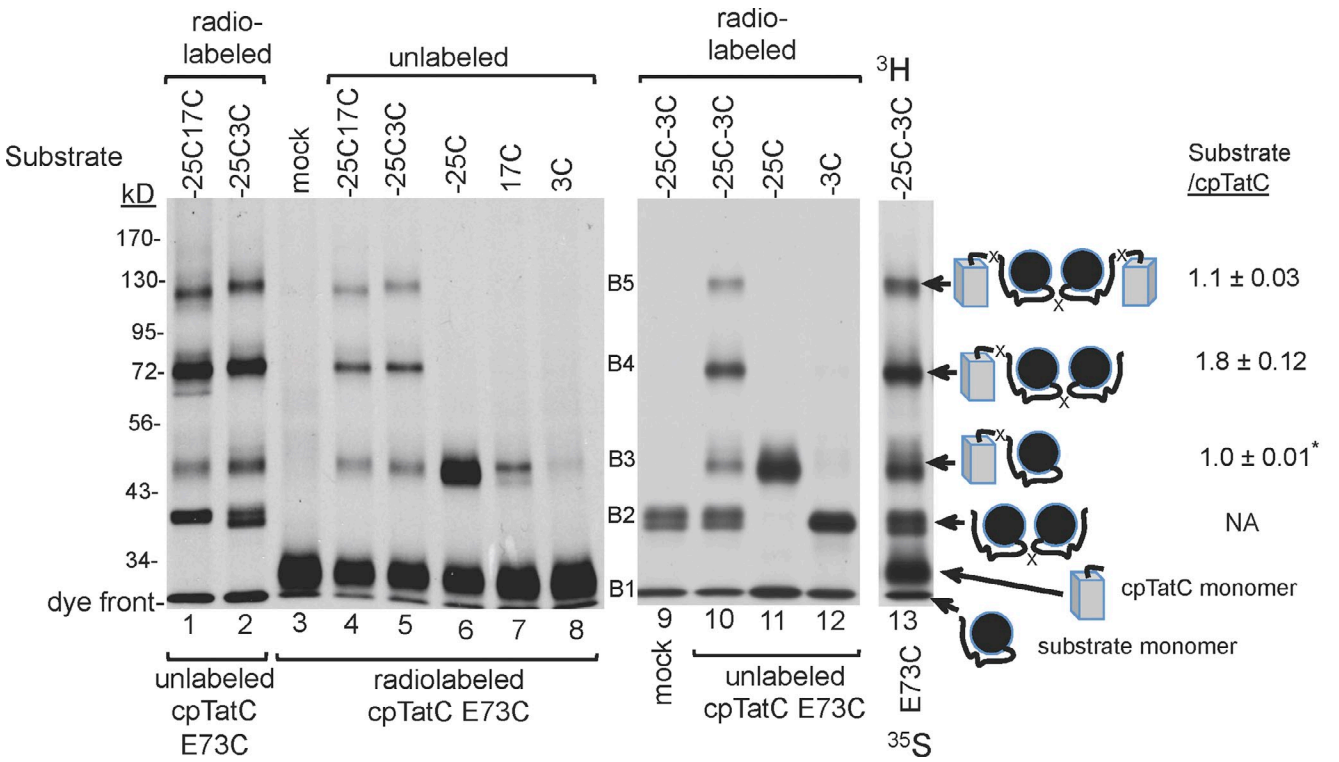

Figure 7. **Substrate protein signal peptides insert between cpTatC subunits.** Thylakoid membranes containing radiolabeled or unlabeled cpTatC E73C (domain S1, shown below the panels) were incubated in a binding reaction with radiolabeled or unlabeled single and double Cys variants of the full-length tOE17-20F substrate as shown above the panels. Disulfide cross-linking was conducted as described in the Materials and methods. The identification of B3 as substrate × cpTatC is inferred from the migration of the cross-linking product between cpTatC E73C and substrate −25C (lanes 6 and 11). The identification of band B2 as substrate dimer is inferred from the migration of the bands from the reaction containing radiolabeled substrate −3C (lane 12). Identification of the B4 band as substrate$_2$ × cpTatC and the B5 band as substrate$_2$ × cpTatC$_2$ was based on their M_r and the substrate/cpTatC abundance in the band. The ratio of abundance was determined in an experiment in which substrate was labeled with ^{3}H-leucine and cpTatC was labeled with ^{35}S-methionine (lane 13). The ratio of tritium to ^{35}S for the B3 band was set as 1:1 (asterisk) and the ratios of B4 and B5 calculated normalized to that value. Ratios are the average and standard deviation obtained from six individual cross-linking assays.

we observed multiple contacts between Tha4 and cpTatC by disulfide cross-linking that fell into three categories; a completely constitutive contact, a contact totally dependent on substrate and the proton gradient, and contacts that, although present constitutively, are enhanced by substrate binding and the proton gradient.

Cross-linking between the cpTatC L3 position T275C and Tha4 TM Cys residues was independent of all three requirements for translocase assembly (Fig. 4, Fig. 5, and Fig. S3 B). Considering that disulfide cross-linking minimally requires diffusion-limited collision within the membrane bilayer, it is certainly possible that the observed cross-linking is not physiologically significant. However, two considerations persuade us that this is a meaningful contact. First, Tha4-cpTatC L3 cross-linking is highly similar to photocrosslinking between *E. coli* TatC and TatA (Zoufaly et al., 2012), which is less likely to capture nonspecific interactions because of the short lifetime of the photoactive group. Both studies detected cross-linking from the cpTatC (TatC) L3 (P3) and L2 (P2) loops to Tha4 (TatA) under constitutive conditions. Second is the efficiency of cross-linking; ∼35% of the cpTatC T275C was cross-linked to Tha4 P9C during a minimal 5-min oxidation period at reduced temperature (Fig. S3). At a minimum, it must be conceded that the L3 site is highly accessible to Tha4.

The association of Tha4 with cpTatC L3 is unlikely to be a strong specific interaction, as Tha4 does not co-purify with the receptor complex (Cline and Mori, 2001) and is not constitutively cross-linked to the receptor complex by the lysine-reactive DSP (dithiobis[succinimidyl propionate]; Mori and Cline, 2002), although the latter result may be due to the absence of lysines in the Tha4 TM and cpTatC L3. Rather, we suspect that the Tha4 TM is close to cpTatC L3 and TM5 because of an association with the Hcf106 TM, which is predicted to bind TM5 by analogy with the TatB TM association with *E. coli* TatC TM5 (Kneuper et al., 2012; Rollauer et al., 2012). The Hcf106 TM domain is 60% identical to, and can functionally substitute for, the Tha4 TM domain (Dabney-Smith et al., 2003), which has been shown to direct Tha4–Tha4 associations independent of E10 (Dabney-Smith and Cline, 2009). A stable TatA–TatB complex has also been reported for the *E. coli* Tat system (Sargent et al., 2001). Based on these considerations, a model for the Tha4 TM and Hcf106 TM positions with respect to cpTatC is presented (Fig. 8 C).

Cross-linking between cpTatC TM4 (L231C) and the Tha4 TM was dependent on all requirements of translocase assembly (Figs. 1, 2, 4, 5, and S3 B), and represents a true translocase contact. Because L231 is topologically adjacent to Q234 (i.e., the comparable residue to *E. coli* TatC E170), this result supports the suggestion by Rollauer et al. (2012) that TatA

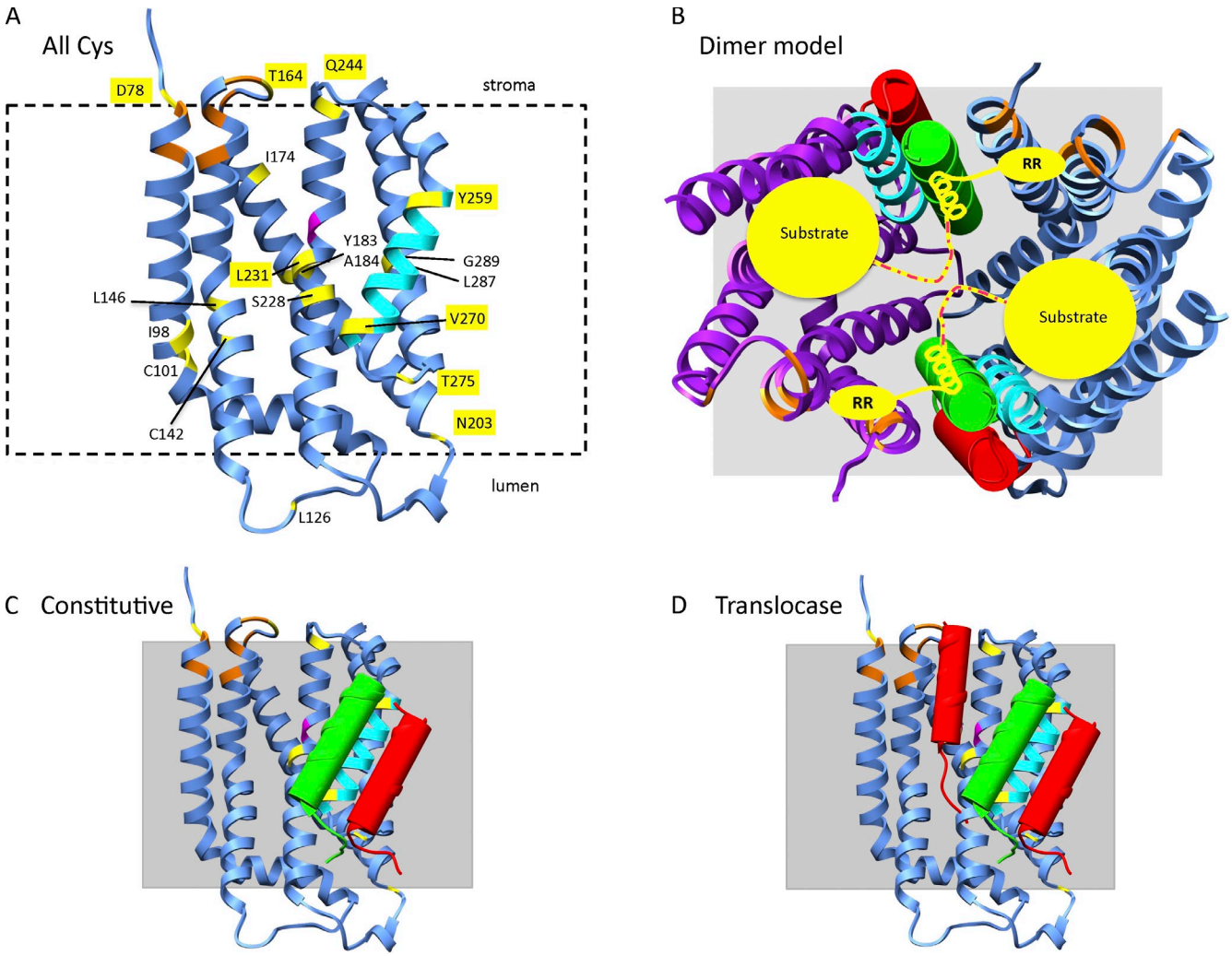

Figure 8. **Models for the association of cpTatC, Tha4, and substrate during assembly of the Tat translocase.** (A) A cartoon model for pea chloroplast TatC structure based on homology with the *A. aeolicus* TatC structure (see Materials and methods) with all Cys substitutions tested in this study colored yellow on the cpTatC backbone and labeled by residue number; yellow highlighted residue numbers produced disulfide cross-links with Tha4. Residues that, when mutated to alanine, impair twin arginine binding are colored orange. Glutamine 234, proposed to mediate docking of Tha4 E10, is colored magenta. The carboxyl-proximal helix of cpTatC TM5 is colored cyan. (B) Proposed arrangement of cpTatC, bound substrates, and the TMs of Tha4 (red cylinders) and Hcf106 (green cylinders) in a dimer of cpTatC. A ribbon depiction of the proposed cpTatC dimer as viewed from the chloroplast stroma with cpTatC subunits colored blue and purple, respectively, is shown. The suggested substrate arrangement is shown in yellow with the signal peptide hydrophobic helix associated with the Hcf106 TM and the carboxyl-proximal signal peptide and N-terminal residues of the substrate mature domain in the central cavity. A stippled yellow line depicts the segment that directs disulfide-linked substrate dimers. (C and D) Interpretation of the positions of Tha4 and Hcf106 TMs with cpTatC constitutively (C) and in the translocase (D) are based on disulfide cross-linking and the position of the *E. coli* TatB (Hcf106 orthologue; Rollauer et al., 2012). The N-terminal segments of Tha4 and Hcf106 were modeled onto the *E. coli* TatA structure (see Materials and methods).

(Tha4) initiates assembly of the transport-active oligomer on the concave face of TatC (cpTatC) by hydrogen bonding of a glutamine–glutamate pair on the partner proteins. Our placement of Tha4 based on the cpTatC L231C and Tha4 P9C cross-linking and alignment of Tha4 E10 with cpTatC Q234 suggests that the Tha4 TM fits in a cleft between cpTatC TM2 and TM4 (Fig. 8 D).

Cross-linking between the Tha4 TM and residues of stroma- and lumen-proximal regions of cpTatC TM5 may be a clue as to how Tha4 enters the cpTatC cavity. These contacts occurred constitutively but increased in the translocase (Fig. 4, Fig. 5, and Fig. S3 B). As shown in Fig. 8 C, constitutively cross-linked Tha4 TM would be very close to both sites on cpTatC TM5. Because the Hcf106 TM probably occupies the TM5 sites, the cross-linking to Tha4 suggests some breathing of the TM5-Hcf106 TM association. The up to fivefold increase in Tha4 TM to cpTatC TM5 cross-linking in the translocase could reflect increased fluctuation of the Hcf106 TM–TM5 association such that Tha4 has increased access to TM5. Alternatively, the increased cross-linking may result from access to TM5 by additional Tha4 subunits assembling in the cavity. The latter scenario might explain the proton gradient requirement for enhanced contact (Fig. 5), as a proton gradient is required for movement of Tha4 into the cpTatC cavity.

A surprising result of these studies is that a large sustained proton gradient is not necessary for initiation of Tha4 assembly (Fig. 5). The effect of ionophores in darkness has been ascribed to a localized pool of protons that do not decay when the light is turned off, but are stripped by ionophores (Dilley, 2004;

Braun and Theg, 2008). Tha4 E10 is a candidate for harboring a localized proton. Topology studies indicate that in unstimulated membranes, E10 is very close to the lumenal face of the thylakoid membrane (Aldridge et al., 2012), consistent with cross-linking between Tha4 P9C and cpTatC T275C. However, for disulfide cross-linking between Tha4 P9C and cpTatC L231C to occur, Tha4 E10 must slide farther toward the center of the bilayer, which would be energetically unfavorable unless E10 is protonated. Movement of Tha4 toward the center of the bilayer would also permit the Tha4 APH to partition more evenly into the membrane interface in the translocase, which was also shown by topology studies (Aldridge et al., 2012).

The arrangement of the bound signal peptide with respect to cpTatC was of interest because signal peptide binding promotes translocase assembly. Recent work (Rollauer et al., 2012; Zoufaly et al., 2012; Ma and Cline, 2013) identified the binding site for the twin arginine motif on cpTatC (TatC) as consisting of a combination of critical residues in the S1 and S2 domains. The extremely high affinity ($K_d \sim 1$ nM) and negligible dissociation of the tOE17-20F substrate (Celedon and Cline, 2012) is largely due to the phenylalanine substitution that produced an optimal RR consensus motif (Gérard and Cline, 2007). This implies that the RR domain for this bound substrate would be tethered to its binding site. Thus, it was interesting that for all of different combinations of H/C domain Cys and cpTatC Cys tested in Fig. 6, the substrate −7C and cpTatC V270C combination was the only one that produced a significant cross-link, suggesting that this region of the bound signal peptide is held in place.

The substrate −7 position and the cpTatC V270 position on the lumen-proximal end of TM5 are particularly relevant with respect to Hcf106. The signal peptide H-domain residues −18 through −9 direct photocrosslinking to Hcf106 (Gérard and Cline, 2006) and the Hcf106 TM is likely bound to cpTatC TM5. A logical extension is that the H-domain binds to the Hcf106 TM and that the −7 position is narrowly exposed to TM5 residue V270 because it is at the end of the Hcf106 interaction domain (Fig. 8 B). The interpretation that the H-domain binds to the Hcf106 TM is consistent with the isolation of suppressors of defective signal peptides that map to the TatB TM (Lausberg et al., 2012) and with photocrosslinking directed from the TatB TM to the substrate (Maurer et al., 2010). A similar conclusion regarding signal peptide binding to the TatB TM was proposed to explain how TatB prevents signal peptide exposure to the periplasmic space (Fröbel et al., 2012). Although the interaction strength is difficult at best to quantify, it appears to significantly contribute to overall substrate binding affinity because introducing a charged residue into the H-domain virtually eliminates substrate binding (Cline and Mori, 2001).

What is puzzling about the above considerations is that distance between the RR binding site and the V270 cross-linking site is ∼30 Å. Although it is possible for the signal peptide to span this distance on a single cpTatC subunit, we think it unlikely. This would require the signal peptide to be largely unstructured and to be exposed to cpTatC residues across a diagonal path connecting the two contacts. However, experimental and predictive evidence suggests a considerable helical content in the signal peptide (San Miguel et al., 2003), and several introduced Cys residues along the diagonal path (I174C, S228C, L231C; Fig. 6) did not cross-link to the signal peptide. An alternative explanation is that the TM5 V270 contact is on a different cpTatC subunit than the one that binds the RR motif. This could occur if cpTatC units are arranged in a head-to-tail configuration. A head-to-tail organization was suggested (Rollauer et al., 2012) to explain the apparent contradiction that, given the 1:1 TatB/TatC stoichiometry, disulfide cross-linking places TatB on TatC TM5 (Rollauer et al., 2012) and photocrosslinking places TatB on the TatC N terminus (Zoufaly et al., 2012).

A head-to-tail arrangement of cpTatC subunits could be either face-to-face or more linear; either would permit the signal peptide RR motif and −7 positions to contact different cpTatC subunits. Despite some uncertainty regarding how tightly the signal peptide RR motif and H-domain are tethered to their binding sites, we think that the face-to-face model can better explain the results in Fig. 7. For a pair of substrates cross-linked to different cpTatC subunits via their RR-proximal regions to be simultaneously cross-linked to each other via their signal peptide −3 residues means that signal peptide residues of the two substrates immediately after the Hcf106 photocrosslinking domain (Gérard and Cline, 2006) are very close to each other. This would be possible with the face-to-face configuration of cpTatC subunits that we propose in Fig. 8 B, but a strictly linear arrangement would place the comparable signal peptide residues as distant as the length of a cpTatC subunit. It is also relevant that the substrate–substrate cross-linking region begins with the signal peptide −7 position and extends into the early mature domain (Fig. 6; Ma and Cline, 2013). Thus, for the situation where substrates saturate the receptor complex, we favor a dimeric face-to-face cpTatC configuration in which the signal peptides and early mature protein residues of both substrates are in the same compartment, i.e., a possibly closed chamber formed by the association of concave cavities of the two cpTatC subunits (Fig. 8 B).

The arrangement of cpTatC subunits in the absence of substrate is less clear and relies on the putative cpTatC dimers directed from the L1 residue L126C and TM5 residue V270C (Fig. 4 C). Both are on the concave face of cpTatC (Fig. 8 A), supporting a face-to-face organization, but in the model of Fig. 8 B appear too far apart to form disulfides. This suggests an offset face-to-face arrangement of the cpTatC subunits that would better align L126 and V270 residues to those on the other subunit. If that is the case, then signal peptide binding to the RR-binding domain and the Hcf106 TM may organize the dimer into the configuration of Fig. 8 B. And, in fact, substrate binding was accompanied by the loss of L126C and V270C directed cpTatC dimerization (Fig. 4 C). This could also explain our previous observation that substrate binding stabilizes the receptor complex to detergent (unpublished data) and blue native–PAGE (Fincher et al., 2003).

The model for cpTatC–cpTatC arrangement proposed (Fig. 8 B) is consistent with the observation that a tandemly fused *E. coli* TatC dimer is functional, even when one (but not both) of the signal peptide–binding sites is mutated (Maldonado et al., 2011), and consistent with a related observation that a TatC mutant impaired in substrate binding can complement a TatC mutant impaired in TatB binding (Buchanan et al., 2002). And it can easily explain the efficient transport of substrate dimers cross-linked

through their early mature domains (Ma and Cline, 2010). The model also suggests some alternative possibilities for how substrate binding might control access of Tha4. The proposed cpTatC–cpTatC arrangement, either in the presence or absence of substrate, would prevent unfettered access of Tha4 to the interior cavities. Insertion of signal peptides and associated mature peptide sequences might raise lateral pressures between the subunits and wedge the edges of the dimer apart. Alternatively, the signal peptide H-domain binding to the Hcf106 TM might counterbalance the attraction of the Hcf106 TM to cpTatC TM5. Any breathing of the cpTatC dimer could transiently detach Hcf106 from TM5 and allow passage of Tha4. This would be consistent with the increased cross-linking of Tha4 to TM5 during translocase assembly. The notion that the constitutively bound Tha4 at T275C passes into the central cavity upon Hcf106 detachment is an attractive possibility, especially if the Tha4 TM is associated with the Hcf106 TM, as this might couple Hcf106 detachment to Tha4 passage. However, we do not presently have evidence that the constitutively associated Tha4 moves into the translocase assembly site.

Our model can explain some aspects of Tat protein transport, but there are many questions to be answered. For instance, the face-to-face cpTatC dimer model doesn't readily explain the efficient transport of disulfide cross-linked substrate tetramers (Ma and Cline, 2010). However, because the tetramers formed much more slowly than substrate dimers, it is possible that the receptor complex with ∼8 copies of cpTatC–Hcf106 rearranges to a tetrameric organization. Tandemly fused tetrameric *E. coli* TatC is active (Maldonado et al., 2011), and cross-linked TatC tetramers have been observed (Zoufaly et al., 2012). Finally, although copurification of Tha4 dimer with cross-linked cpTatC L231C (Fig. 2) implies a Tha4 oligomer at the internal site, this needs to be rigorously demonstrated. Nevertheless, our studies provide an experimentally testable model, and such experiments will lead to further refinement of translocase and transport models for this remarkable translocation system.

Materials and methods

Generation of cysteine-substituted cpTatC and Tha4 and truncated substrate proteins

DNA constructs encoding single Cys-substituted Tha4 (Tha4(XnC)) were generated by QuikChange mutagenesis (Agilent Technologies) according to the manufacturer's instructions. The template used for mutagenesis was the coding sequence for mature Tha4 from pea (*Pisum sativum*; GenBank accession no. AAD33943) lacking the chloroplast targeting peptide; the protein sequence begins with "MAFFGLGVPE…" (Fincher et al., 2003) and is labeled starting with the N-terminal methionine as position 1. All Tha4 constructs were cloned into pGEM4Z (Promega). All cpTatC constructs were prepared from pSSU13pre-cpTatC, which was constructed by splice overlap extension (Horton et al., 1989) and contains the transit peptide and first 13 residues of the mature domain of the pea (*P. sativum*) small subunit of ribulose-1,5-bis-phosphate carboxylase/oxygenase (GenBank accession no. AAA33685), fused to the N terminus of the complete precursor sequence for pea (*P. sativum*) cpTatC (GenBank accession no. AAK93948; Ma and Cline, 2013), and cloned into pGEM4Z. For simplicity, pSSU13pre-cpTatC will be referred to in this publication as pre-cpTatC. The His-tagged pre-cpTatC precursor was constructed by splice overlap extension with the coding sequence for GGGGSGGGGSGGGGSHHHHHH fused to the pre-cpTatC C terminus (Ma and Cline, 2013). All cpTatC constructs are numbered from the start of the mature cpTatC sequence, which begins with "CFAVDDEIRE…". All Cys variants of cpTatC were made by QuikChange mutagenesis with, as template, pre-cpTatCaaa (with or without the C-terminal His tag), a variant of pre-cpTatC with all natural Cys residues substituted by alanine (Ma and Cline, 2013).

The tOE17-20F substrate protein is a modified form of the OE17 precursor protein from maize (GenBank accession no. Q41048), which lacks the chloroplast transit peptide and several nonessential residues of the thylakoid-targeting signal peptide. It also contains a phenylalanine at the twin-arginine (RR) +2 position, resulting in higher affinity binding (Ma and Cline, 2000; Gérard and Cline, 2007). The clone for tOE17-20F (Gérard and Cline, 2007) was used as template to prepare by QuikChange single and double Cys-substituted substrates as well as truncated substrate proteins SpF8 through SpF29, where the number after the SpF refers to the number of mature domain residues after the signal peptide. For a subset of substrates, as specifically designated in the text and figure legends, the thylakoid-processing peptidase cleavage site, ala-arg-ala (ARA), was substituted with ala-arg-thr (ART), resulting in noncleavable substrate proteins. All clones, including those with nucleotide changes produced by PCR-based techniques, were sequenced by the Interdisciplinary Center for Biotechnology Research DNA Sequencing Core Facility of the University of Florida.

Capped mRNAs were transcribed in vitro with SP6 polymerase (Promega) and were translated in vitro in the presence of ^{3}H-leucine, the full complement of unlabeled amino acids, or ^{35}S-methionine with a homemade wheat germ translation system (Cline, 1986). Translations were diluted 1:1 and adjusted to import buffer (50 mM Hepes/KOH, pH 8.0, and 0.33 M sorbitol) containing 30 mM leucine or 30 mM methionine as appropriate before use in assays. Translation reactions for substrates and/or Tha4 were treated with apyrase at 6 units per 100 µl undiluted translation product for at least 2 h on ice to deplete them of ATP and ADP.

Antibodies

Antibodies were prepared in rabbits by Cocalico Biologicals, Inc., against the following antigens. The Tha4 and Hcf106 antigens were the amphipathic helix and unstructured carboxyl tail of *P. sativum* Tha4 and *P. sativum* Hcf106, respectively, expressed in *E. coli* with N-terminal histidine tags and purified with Ni-NTA Sepharose (GE Healthcare; Mori et al., 1999, 2001). The antigen for cpTatC was the first 116 residues of *P. sativum* pre-cpTatC, which contained the transit peptide and first stroma-exposed segment, expressed as an N-terminal GST fusion protein expressed in *E. coli* and purified with glutathione-Sepharose (GE Healthcare; Mori et al., 2001). The antigen for psAlb3 (previously called cpOxa1) was the C-terminal soluble domain (residues 305–442) of the *P. sativum* Alb3 orthologue (GenBank accession no. CAA73179) expressed with an N-terminal histidine tag in *E. coli* and purified with Ni-NTA Sepharose (Cline and Mori, 2001).

Source plants, chloroplast and thylakoid isolation, and chloroplast import assays

Intact chloroplasts were isolated from 9–10-d-old pea seedlings (cv. Little Marvel) and were resuspended in import buffer (Cline et al., 1993). Chlorophyll concentrations were determined according to Arnon (1949). Radiolabeled or unlabeled in vitro–translated pre-cpTatC was incubated with chloroplasts (0.33 mg chlorophyll/ml) and 5 mM Mg-ATP in import buffer with ∼100 µE/m^2/s of white light in a 25°C water bath for 40 min. After import, intact chloroplasts were re-purified by centrifugation through 35% Percoll in import buffer and washed with import buffer (Cline et al., 1993). Where stated, chloroplasts were treated with the protease thermolysin before re-purification through 35% Percoll in import buffer containing 5 mM EDTA (Cline et al., 1993). Thylakoid membranes were prepared from the chloroplasts by osmotic lysis and centrifugation as above and resuspended in import buffer containing 5 mM $MgCl_2$.

Functional tests for modified proteins

All modified substrate proteins were tested in binding assays and transport assays. In general, radiolabeled in vitro–translated substrates were incubated with thylakoids in darkness at 0°C for 10–30 min, and the substrate-bound thylakoids were recovered and washed twice with a change of microfuge tubes. For transport assays, radiolabeled in vitro–translated substrate was incubated with thylakoids for 20 min at 25°C in the light. The amounts of substrate binding and substrate transport were quantified by scintillation counting of extracted gel bands (Cline, 1986). All Tha4 variants were previously tested for their ability to facilitate protein transport (Dabney-Smith et al., 2003, 2006; Dabney-Smith and Cline, 2009; Aldridge et al., 2012). Basically, this assay used thylakoids inactivated for endogenous Tha4 with anti-Tha4 antibodies and protein A, followed by in vitro integration of in vitro–translated test Tha4(XnC) and assay for transport of in vitro–translated substrate DT23.

Functionality of Cys-substituted cpTatC for binding and transport was determined as described previously (Ma and Cline, 2013) and is shown in Figs. S2 and S4 as follows. Radiolabeled single Cys variants of pre-cpTatCaaa were imported into chloroplasts. Re-purified chloroplasts were used to prepare thylakoid membranes, which were quantified for chlorophyll content (Arnon, 1949). Equivalent amounts of thylakoids were incubated with radiolabeled substrate tOE17-20F for binding assays on ice for 30 min. Thylakoids from a mock import assay were also used for substrate binding. Portions of doubly washed thylakoids from binding reactions were further incubated in chase assays that contained in vitro–translated Tha4 and a stoichiometric amount of stromal extract for 30 min at 25°C in 70–100 μE/m^2/s of white light. Samples were analyzed by SDS-PAGE/fluorography and the radioactivity in substrate, transported substrate, and cpTatC bands was quantified by scintillation counting of extracted gel bands (Celedon and Cline, 2012). The increase in bound substrate due to the imported cpTatC is expressed as substrate bound per imported cpTatC (i.e., Δ binding/imported cpTatC). Percentages of substrates bound per imported cpTatC that were transported in the chase assay are displayed. These percentages were calculated by subtracting the bound precursor and chased precursor in the mock import thylakoids from those obtained with thylakoids containing imported cpTatC, i.e., Δchase/Δbinding as described by Ma and Cline (2013). Dithiothreitol was included in all buffers and assay mixtures at 2 mM.

Disulfide cross-linking between imported cpTatC and Tha4

Radiolabeled single Cys-substituted pre-cpTatCaaa was imported into chloroplasts, the chloroplasts treated with thermolysin and then re-purified. Thylakoids (~25 μg of chlorophyll in 25 μl import buffer, 5 mM $MgCl_2$) obtained from the chloroplasts were incubated with 25 μl in vitro–translated and apyrase-treated unlabeled Tha4 or with mock translation extract for 10 min at 15°C in the light (~35 μE/m^2/s). In vitro–translated apyrase-treated substrate (50 μl) was added and the reaction mixture was incubated in darkness at 0°C for 10 min. Samples were warmed to 15°C in darkness for 3 min and transferred to a 15°C illuminated water bath (~70 μE/m^2/s white light) to initiate translocase assembly. After 2.5–3 min, disulfide formation was initiated with 2 mM CuP oxidant (Dabney-Smith et al., 2006). Reactions were terminated after 5 min by addition of 2 vol of import buffer, containing 14 mM EDTA and 25 mM *N*-ethylmaleimide, which inactivates all disulfides within 10 s of addition. Recovered thylakoids were dissolved in SDS sample buffer that contained 8 M urea without reducing agent by incubation at room temperature for 60 min. Samples were analyzed by 10% SDS-PAGE and fluorography. For reduction of disulfide bonds, samples in SDS sample buffer received 10% β-mercaptoethanol by volume.

Disulfide cross-linking of Cys-substituted substrates

Single Cys-substituted pre-cpTatCaaa was imported into chloroplasts and thylakoids isolated as above with the exception that, after lysis, thylakoids were resuspended in import buffer, 5 mM $MgCl_2$, and 2 mM dithiothreitol. Recovered thylakoids (~25 μg of chlorophyll) were incubated with 25 μl in vitro–translated and apyrase-treated Cys-substituted substrate for 20 min on ice. Thylakoids were recovered and washed once with 200 μl import buffer, 5 mM $MgCl_2$, and 2 mM dithiothreitol, and resuspended in 100 μl import buffer and 5 mM $MgCl_2$. After 3 min at 15°C, assays were treated with 2 mM CuP for 5 min and terminated as described above.

Cys–Cys cross-linking with BMOE

For the experiments shown in Fig. 4 and Fig. S5, Cys residues were cross-linked with the irreversible cross-linker BMOE. Conditions were similar to disulfide cross-linking (above), except that thylakoids were resuspended in import buffer and 0.5 mM Tris(2-carboxyethyl)phosphine hydrochloride (TCEP), reactions were conducted in the same buffer, and cross-linking was initiated with 1 mM of the BMOE, aliquoted from a 40 mM stock in dimethylsulfoxide. Reactions at 25°C were terminated after 10 min with 20 mM dithiothreitol.

Cross-linking with DSP

Reaction mixtures contained 35 μg chlorophyll of thylakoids or substrate-bound thylakoids, 5 mM Mg-ATP, 10 μM methylviologen in import buffer, 3.3 mM $MgCl_2$ and, where indicated, 1 μM of bacterially expressed tOE23 substrate added immediately before transferring reaction mixtures to a 25°C bath illuminated with ~100 μE/m^2/s white light. After 5 min the DSP was added to 1 mM from a 50-mM stock in dimethylsulfoxide. Cross-linking was terminated after 5 min with 10 mM Tris-HCl, pH 7.6, as described previously (Mori and Cline, 2002).

Co-immunoprecipitation of cross-linked complexes

After cross-linking, thylakoid samples were denatured with 1% SDS, 50 mM Tris-HCl, pH 7.6, 150 mM NaCl, and 0.5 mM EDTA for 10 min at 37°C, briefly centrifuged, diluted with 12.5 vol of immunoprecipitation buffer (50 mM Tris-HCl, pH 7.6, 150 mM NaCl, 0.1 mM EDTA, 1% Triton X-100, and 0.5% deoxycholate), and subjected to immunoprecipitation (Mori and Cline, 2002). In brief, 60 μl of a 25% suspension of IgGs covalently cross-linked to protein A–Sepharose (GE Healthcare; Mori and Cline, 2002) were added to the solubilized samples and the resulting suspension was mixed end-over-end at 4°C for 3 h. The beads were washed three times with immunoprecipitation buffer and bound protein was eluted with 38 μl 5% SDS, 8 M urea, and 0.25 M Tris-HCl, pH 6.8, for 1 h at 37°C. The beads were removed by centrifugation. For samples cross-linked with DSP, the eluates were reduced with 10% β-mercaptoethanol by volume for 1 h at room temperature to break the cross-linker. Disulfide cross-linked samples were either analyzed directly or first reduced with β-mercaptoethanol before analysis. For immunoblotting, SDS-PAGE gels were electroblotted to 0.2-μm pore-sized nitrocellulose membranes. After incubation with antibodies, the blots were developed with the ECL method (GE Healthcare).

Metal ion affinity purification of Tha4-cpTatC His_6 disulfide cross-linked complexes

Washed thylakoids from cysteine cross-linking reactions were resuspended at 1 mg of chlorophyll/ml in solubilization buffer (0.25× import buffer, 20% glycerol, and 0.5 M amino-caproic acid) containing 1% digitonin and 1 mM PMSF. The samples were incubated on ice for 1 h and then centrifuged at 150,000 *g* at 2°C for 30 min. The supernatants were adjusted to binding buffer (20 mM Hepes, pH 7.8, 150 mM NaCl, and 20 mM imidazole) and mixed with Ni-NTA magnetic beads (QIAGEN) end-over-end for ≥4 h at 4°C. The beads were washed with binding buffer containing 0.2% digitonin and the bound proteins were eluted with 0.5× binding buffer containing 100 mM EDTA and 0.2% digitonin as described previously (Ma and Cline, 2013). Samples were either analyzed directly or after reducing with β-mercaptoethanol.

Model for the structure of cpTatC from *P. sativum*

The sequence of cpTatC from *P. sativum* (GenBank accession no. AAK93948) was homology modeled onto the three-dimensional structure of the *A. aeolicus* TatC protein (Protein Data Bank accession no. 4HTT; Ramasamy et al., 2013) using the MODELLER tool of Chimera (Pettersen et al., 2004; Eswar et al., 2006), guided by an alignment between the last 230 amino acids of pea cpTatC and the sequence of *A. aeolicus* TatC (Protein Data Bank accession no. 4B4A_A). The N-terminal 21 residues ("AFFGLGVPELVVI-AGVAALVF") of the *P. sativum* mature Tha4 (GenBank accession no. AAD33943) and the 22 N-terminal residues ("ASLFGVGAPEALVIGV-VALLVF") of the *P. sativum* mature Hcf106 (GenBank accession no. AAK93949) were modeled onto the structure of *E. coli* TatA (PDB 2LZR) guided by the alignment with the sequence of TatA (Protein Data Bank accession no. 2LZR_A). The "PipesAndPlanks" tool of Chimera was used for the cylindrical depiction of the TM helices of Tha4 and Hcf106. Alignments were conducted by Multalin (http://multalin.toulouse.inra.fr/multalin/multalin.html).

Experimental replicates

All experiments were repeated at least two times. Unless otherwise noted in the figure legends, the data shown are from a single representative experiment.

Online supplemental material

Supplementary figures support the results presented in the main manuscript. Fig. S1 documents the use of truncated precursors to stably assemble the translocase without being transported. Fig. S2 measures the functionality of most Cys-substituted cpTatC used here for binding and transport. Fig. S3 provides an estimate for the disulfide cross-linking yield for each cpTatC-Tha4 pair and also estimates the substrate enhancement of cross-linking. Fig. S4 shows the cross-linking between Tha4 P9C and cpTatC with single Cys substitutions in TM domains presenting on the concave face of cpTatC. Fig. S5 demonstrates that a substrate/cpTatC adduct multiply cross-linked via RR-binding sites and the substrate dimerization region is functional for protein translocation. Online supplemental material is available at http://www.jcb.org/cgi/content/full/jcb.201311057/DC1.

K. Cline is grateful to B. Berks for suggesting that Tha4 (TatA) might assemble in the interior of a cpTatC (TatC) oligomer and to M. Settles for his insightful comments. We thank Y. Li and M. McCaffery for critical review of the manuscript. We also thank M. McCaffery for excellent technical assistance.

This work was supported in part by National Institutes of Health grant R01 GM46951 (to K. Cline).

The authors declare no competing financial interests.

Submitted: 14 November 2013
Accepted: 11 March 2014

References

Alami, M., I. Lüke, S. Deitermann, G. Eisner, H.G. Koch, J. Brunner, and M. Müller. 2003. Differential interactions between a twin-arginine signal peptide and its translocase in *Escherichia coli*. *Mol. Cell*. 12:937–946. http://dx.doi.org/10.1016/S1097-2765(03)00398-8

Alcock, F., M.A. Baker, N.P. Greene, T. Palmer, M.I. Wallace, and B.C. Berks. 2013. Live cell imaging shows reversible assembly of the TatA component of the twin-arginine protein transport system. *Proc. Natl. Acad. Sci. USA*. 110:E3650–E3659. http://dx.doi.org/10.1073/pnas.1306738110

Alder, N.N., and S.M. Theg. 2003. Energetics of protein transport across biological membranes. a study of the thylakoid DeltapH-dependent/cpTat pathway. *Cell*. 112:231–242. http://dx.doi.org/10.1016/S0092-8674(03)00032-1

Aldridge, C., A. Storm, K. Cline, and C. Dabney-Smith. 2012. The chloroplast twin arginine transport (Tat) component, Tha4, undergoes conformational changes leading to Tat protein transport. *J. Biol. Chem.* 287:34752–34763. http://dx.doi.org/10.1074/jbc.M112.385666

Arnon, D.I. 1949. Copper enzymes in isolated chloroplasts. Polyphenol oxidase in *Beta vulgaris*. *Plant Physiol.* 24:1–15. http://dx.doi.org/10.1104/pp.24.1.1

Braun, N.A., and S.M. Theg. 2008. The chloroplast Tat pathway transports substrates in the dark. *J. Biol. Chem.* 283:8822–8828. http://dx.doi.org/10.1074/jbc.M708948200

Buchanan, G., E. de Leeuw, N.R. Stanley, M. Wexler, B.C. Berks, F. Sargent, and T. Palmer. 2002. Functional complexity of the twin-arginine translocase TatC component revealed by site-directed mutagenesis. *Mol. Microbiol.* 43:1457–1470. http://dx.doi.org/10.1046/j.1365-2958.2002.02853.x

Celedon, J.M., and K. Cline. 2012. Stoichiometry for binding and transport by the twin arginine translocation system. *J. Cell Biol.* 197:523–534. http://dx.doi.org/10.1083/jcb.201201096

Celedon, J.M., and K. Cline. 2013. Intra-plastid protein trafficking: how plant cells adapted prokaryotic mechanisms to the eukaryotic condition. *Biochim. Biophys. Acta*. 1833:341–351. http://dx.doi.org/10.1016/j.bbamcr.2012.06.028

Cline, K. 1986. Import of proteins into chloroplasts. Membrane integration of a thylakoid precursor protein reconstituted in chloroplast lysates. *J. Biol. Chem.* 261:14804–14810.

Cline, K., and H. Mori. 2001. Thylakoid DeltapH-dependent precursor proteins bind to a cpTatC-Hcf106 complex before Tha4-dependent transport. *J. Cell Biol.* 154:719–729. http://dx.doi.org/10.1083/jcb.200105149

Cline, K., R. Henry, C. Li, and J. Yuan. 1993. Multiple pathways for protein transport into or across the thylakoid membrane. *EMBO J.* 12:4105–4114.

Dabney-Smith, C., and K. Cline. 2009. Clustering of C-terminal stromal domains of Tha4 homo-oligomers during translocation by the Tat protein transport system. *Mol. Biol. Cell*. 20:2060–2069. http://dx.doi.org/10.1091/mbc.E08-12-1189

Dabney-Smith, C., H. Mori, and K. Cline. 2003. Requirement of a Tha4-conserved transmembrane glutamate in thylakoid Tat translocase assembly revealed by biochemical complementation. *J. Biol. Chem.* 278:43027–43033. http://dx.doi.org/10.1074/jbc.M307923200

Dabney-Smith, C., H. Mori, and K. Cline. 2006. Oligomers of Tha4 organize at the thylakoid Tat translocase during protein transport. *J. Biol. Chem.* 281:5476–5483. http://dx.doi.org/10.1074/jbc.M512453200

Dilley, R.A. 2004. On why thylakoids energize ATP formation using either delocalized or localized proton gradients - a ca(2+) mediated role in thylakoid stress responses. *Photosynth. Res.* 80:245–263. http://dx.doi.org/10.1023/B:PRES.0000030436.32486.aa

Eswar, N., B. Webb, M.A. Marti-Renom, M.S. Madhusudhan, D. Eramian, M.Y. Shen, U. Pieper, and A. Sali. 2006. Comparative protein structure modeling using Modeller. *Curr. Protoc. Bioinformatics*. Chapter 5:Unit 5.6.

Fincher, V., C. Dabney-Smith, and K. Cline. 2003. Functional assembly of thylakoid deltapH-dependent/Tat protein transport pathway components in vitro. *Eur. J. Biochem.* 270:4930–4941. http://dx.doi.org/10.1046/j.1432-1033.2003.03894.x

Fröbel, J., P. Rose, and M. Müller. 2011. Early contacts between substrate proteins and TatA translocase component in twin-arginine translocation. *J. Biol. Chem.* 286:43679–43689. http://dx.doi.org/10.1074/jbc.M111.292565

Fröbel, J., P. Rose, F. Lausberg, A.S. Blümmel, R. Freudl, and M. Müller. 2012. Transmembrane insertion of twin-arginine signal peptides is driven by TatC and regulated by TatB. *Nat Commun*. 3:1311. http://dx.doi.org/10.1038/ncomms2308

Gérard, F., and K. Cline. 2006. Efficient twin arginine translocation (Tat) pathway transport of a precursor protein covalently anchored to its initial cpTatC binding site. *J. Biol. Chem.* 281:6130–6135. http://dx.doi.org/10.1074/jbc.M512733200

Gérard, F., and K. Cline. 2007. The thylakoid proton gradient promotes an advanced stage of signal peptide binding deep within the Tat pathway receptor complex. *J. Biol. Chem.* 282:5263–5272. http://dx.doi.org/10.1074/jbc.M610337200

Horton, R.M., H.D. Hunt, S.N. Ho, J.K. Pullen, and L.R. Pease. 1989. Engineering hybrid genes without the use of restriction enzymes: gene splicing by overlap extension. *Gene*. 77:61–68. http://dx.doi.org/10.1016/0378-1119(89)90359-4

Hu, Y., E. Zhao, H. Li, B. Xia, and C. Jin. 2010. Solution NMR structure of the TatA component of the twin-arginine protein transport system from gram-positive bacterium Bacillus subtilis. *J. Am. Chem. Soc.* 132:15942–15944. http://dx.doi.org/10.1021/ja1053785

Klein, M.J., S.L. Grage, C. Muhle-Goll, J. Bürck, S. Afonin, and A.S. Ulrich. 2012. Structure analysis of the membrane-bound PhoD signal peptide of the Tat translocase shows an N-terminal amphiphilic helix. *Biochim. Biophys. Acta*. 1818:3025–3031. http://dx.doi.org/10.1016/j.bbamem.2012.08.002

Kneuper, H., B. Maldonado, F. Jäger, M. Krehenbrink, G. Buchanan, R. Keller, M. Müller, B.C. Berks, and T. Palmer. 2012. Molecular dissection of TatC defines critical regions essential for protein transport and a TatB-TatC contact site. *Mol. Microbiol.* 85:945–961. http://dx.doi.org/10.1111/j.1365-2958.2012.08151.x

Koch, S., M.J. Fritsch, G. Buchanan, and T. Palmer. 2012. *Escherichia coli* TatA and TatB proteins have N-out, C-in topology in intact cells. *J. Biol. Chem.* 287:14420–14431. http://dx.doi.org/10.1074/jbc.M112.354555

Lausberg, F., S. Fleckenstein, P. Kreutzenbeck, J. Fröbel, P. Rose, M. Müller, and R. Freudl. 2012. Genetic evidence for a tight cooperation of TatB and TatC during productive recognition of twin-arginine (Tat) signal peptides in *Escherichia coli*. *PLoS ONE*. 7:e39867. http://dx.doi.org/10.1371/journal.pone.0039867

Leake, M.C., N.P. Greene, R.M. Godun, T. Granjon, G. Buchanan, S. Chen, R.M. Berry, T. Palmer, and B.C. Berks. 2008. Variable stoichiometry of the TatA component of the twin-arginine protein transport system observed by in vivo single-molecule imaging. *Proc. Natl. Acad. Sci. USA*. 105:15376–15381. http://dx.doi.org/10.1073/pnas.0806338105

Lee, P.A., G.L. Orriss, G. Buchanan, N.P. Greene, P.J. Bond, C. Punginelli, R.L. Jack, M.S. Sansom, B.C. Berks, and T. Palmer. 2006. Cysteine-scanning mutagenesis and disulfide mapping studies of the conserved domain of the twin-arginine translocase TatB component. *J. Biol. Chem.* 281:34072–34085. http://dx.doi.org/10.1074/jbc.M607295200

Ma, X., and K. Cline. 2000. Precursors bind to specific sites on thylakoid membranes prior to transport on the delta pH protein translocation system. *J. Biol. Chem.* 275:10016–10022. http://dx.doi.org/10.1074/jbc.275.14.10016

Ma, X., and K. Cline. 2010. Multiple precursor proteins bind individual Tat receptor complexes and are collectively transported. *EMBO J.* 29:1477–1488. http://dx.doi.org/10.1038/emboj.2010.44

Ma, X., and K. Cline. 2013. Mapping the signal peptide binding and oligomer contact sites of the core subunit of the pea twin arginine protein translocase. *Plant Cell*. 25:999–1015. http://dx.doi.org/10.1105/tpc.112.107409

Ma, C., G. Agrawal, and S. Subramani. 2011. Peroxisome assembly: matrix and membrane protein biogenesis. *J. Cell Biol.* 193:7–16. http://dx.doi.org/10.1083/jcb.201010022

Maldonado, B., G. Buchanan, M. Müller, B.C. Berks, and T. Palmer. 2011. Genetic evidence for a TatC dimer at the core of the *Escherichia coli* twin arginine (Tat) protein translocase. *J. Mol. Microbiol. Biotechnol.* 20:168–175. http://dx.doi.org/10.1159/000329076

Maurer, C., S. Panahandeh, A.C. Jungkamp, M. Moser, and M. Müller. 2010. TatB functions as an oligomeric binding site for folded Tat precursor proteins. *Mol. Biol. Cell*. 21:4151–4161. http://dx.doi.org/10.1091/mbc.E10-07-0585

Mori, H., and K. Cline. 2002. A twin arginine signal peptide and the pH gradient trigger reversible assembly of the thylakoid [Delta]pH/Tat translocase. *J. Cell Biol.* 157:205–210. http://dx.doi.org/10.1083/jcb.200202048

Mori, H., E.J. Summer, X. Ma, and K. Cline. 1999. Component specificity for the thylakoidal Sec and Delta pH-dependent protein transport pathways. *J. Cell Biol.* 146:45–56. http://dx.doi.org/10.1083/jcb.146.1.45

Mori, H., E.J. Summer, and K. Cline. 2001. Chloroplast TatC plays a direct role in thylakoid (Delta)pH-dependent protein transport. *FEBS Lett.* 501:65–68. http://dx.doi.org/10.1016/S0014-5793(01)02626-6

Pal, D., K. Fite, and C. Dabney-Smith. 2013. Direct interaction between a precursor mature domain and transport component Tha4 during twin arginine transport of chloroplasts. *Plant Physiol.* 161:990–1001. http://dx.doi.org/10.1104/pp.112.207522

Palmer, T., and B.C. Berks. 2012. The twin-arginine translocation (Tat) protein export pathway. *Nat. Rev. Microbiol*. 10:483–496. http://dx.doi.org/10.1038/nrmicro2814

Pettersen, E.F., T.D. Goddard, C.C. Huang, G.S. Couch, D.M. Greenblatt, E.C. Meng, and T.E. Ferrin. 2004. UCSF Chimera—a visualization system for exploratory research and analysis. *J. Comput. Chem.* 25:1605–1612. http://dx.doi.org/10.1002/jcc.20084

Ramasamy, S., R. Abrol, C.J. Suloway, and W.M. Clemons Jr. 2013. The glove-like structure of the conserved membrane protein TatC provides insight into signal sequence recognition in twin-arginine translocation. *Structure*. 21:777–788. http://dx.doi.org/10.1016/j.str.2013.03.004

Rodriguez, F., S.L. Rouse, C.E. Tait, J. Harmer, A. De Riso, C.R. Timmel, M.S. Sansom, B.C. Berks, and J.R. Schnell. 2013. Structural model for the protein-translocating element of the twin-arginine transport system. *Proc. Natl. Acad. Sci. USA*. 110:E1092–E1101. http://dx.doi.org/10.1073/pnas.1219486110

Rollauer, S.E., M.J. Tarry, J.E. Graham, M. Jääskeläinen, F. Jäger, S. Johnson, M. Krehenbrink, S.M. Liu, M.J. Lukey, J. Marcoux, et al. 2012. Structure of the TatC core of the twin-arginine protein transport system. *Nature*. 492:210–214. http://dx.doi.org/10.1038/nature11683

Rose, P., J. Fröbel, P.L. Graumann, and M. Müller. 2013. Substrate-dependent assembly of the Tat translocase as observed in live *Escherichia coli* cells. *PLoS ONE*. 8:e69488. http://dx.doi.org/10.1371/journal.pone.0069488

San Miguel, M., R. Marrington, P.M. Rodger, A. Rodger, and C. Robinson. 2003. An *Escherichia coli* twin-arginine signal peptide switches between helical and unstructured conformations depending on the hydrophobicity of the environment. *Eur. J. Biochem.* 270:3345–3352. http://dx.doi.org/10.1046/j.1432-1033.2003.03710.x

Sargent, F., U. Gohlke, E. De Leeuw, N.R. Stanley, T. Palmer, H.R. Saibil, and B.C. Berks. 2001. Purified components of the *Escherichia coli* Tat protein transport system form a double-layered ring structure. *Eur. J. Biochem.* 268:3361–3367. http://dx.doi.org/10.1046/j.1432-1327.2001.02263.x

Zoufaly, S., J. Fröbel, P. Rose, T. Flecken, C. Maurer, M. Moser, and M. Müller. 2012. Mapping precursor-binding site on TatC subunit of twin arginine-specific protein translocase by site-specific photo cross-linking. *J. Biol. Chem.* 287:13430–13441. http://dx.doi.org/10.1074/jbc.M112.343798